Design and Development of the Magnetorheological Honing Process

A Dissertation Submitted
In Partial Fulfillment of the Requirements
for the Degree of

Master of Engineering

in

CAD/CAM and Robotics

by

Nitin Chawla

to the

MECHANICAL ENGINEERING DEPARTMENT
THAPAR UNIVERSITY, PATIALA

July, 2015

CERTIFICATE

I hereby declare that the thesis entitled **"Design and development of the magnetorheological honing process"** is an authentic record of my study carried out as requirements for the award of the degree of **Master of Engineering** in **CAD/CAM and Robotics** at **Thapar University, Patiala** under the supervision of **Dr. Anant Kumar Singh**, Assistant Professor, Mechanical Engineering Department, Thapar University, Patiala during July, 2015. The matter embodied in this report has not been submitted in partial or full to any other university or institute for the award of any degree.

Date: 15/07/2015

Nitin Chawla

Roll no: 801381012

It is certified that the above statement made by the student is correct to the best of my/our knowledge and belief.

14/07/2015

Dr. Anant Kumar Singh
Assistant Professor
Mechanical Engineering Department
Thapar University, Patiala - 147004

Countersigned by

Dr. S. K. Mohapatra
Professor & Head
Mechanical Engineering Department
Thapar University, Patiala – 147004

Dr. S.S Bhatia
Dean of Academic Affairs
Thapar University, Patiala - 147004

ii

Acknowledgements

I am highly grateful to the authorities of Thapar University, Patiala for providing this opportunity to carry out the report work.

I would like to express a deep sense of gratitude and thank profusely to my thesis guide **Dr. Anant Kumar Singh** for their sincere & invaluable guidance and suggestions which inspired me to submit thesis report in the present form.
I would also like to thank all the faculty members of Mechanical engineering department for their intellectual support and unyielding encouragement.

I am deeply indebted to all my friends who helped me with their encouragement, ample morale support and valuable suggestions.

Finally, I would like to extend my gratitude to Talwinder Singh Bedi, Akshay khurana, Vishwas Grover, Prince Garg and all those who directly or indirectly helped me in the process and contributed towards this phase of my report work.

Nitin Chawla

Abstract

A new precise finishing process i.e. magnetorheological honing process for finishing of internal surfaces of cylindrical work material is developed. A computer controlled experimental setup is designed and developed for finishing of both ferromagnetic and non-ferromagnetic work material using smart fluid named as magnetorheological polishing fluid. The MRP fluid consists of base fluid, carbonyl iron particles and abrasive particles. For the initial stage a mounting bracket is designed and analyzed for holding the servomotor and tool holder shaft. Static structural and modal analysis for the bracket was done in the Workbench 14.5 software. Stresses and total deformation acting on the bracket assembly were calculated in the static structural analysis. Frequencies at different mode shapes were calculated in the Modal analysis under the initial boundary conditions. Length of the tool holder shaft was decided on the basis of modal analysis done in Workbench 14.5 software (student version). CAD model of each part was created in the CREO 5.0 software (student version). Dimensions of the magnetorheological honing tool were decided on the basis of maximum magnetic flux density distribution at the outer surface of the tool.

The preliminary experimentation was carried out on both mild steel and aluminium workpiece in order to investigate the effect of finishing time on the value of surface roughness. The initial average roughness value of ferromagnetic workpiece was 1.90 μm whereas for the aluminium workpiece was 3.25 μm. SEM analysis was also carried out in order to determine the surface morphology before/after finishing. From experimentations, it is concluded that the newly developed magnetorheological honing process has the capability to do surface finishing of internal surfaces of both ferromagnetic and non ferromagnetic work surfaces. The developed process has its likely applications in manufacturing and automotive industry.

Contents

List of Figures

List of Tables

Nomenclature

Ra	centre line average roughness value (µm)
Rz	peak roughness value (µm)
Rq	RMS roughness value (µm)
F_f	finishing force (N)
F_n	normal force (N)
F_s	shear force (N)
E	young's modulus
√	poisson's ratio
L	length of the belt (mm)
C	centre distance between the two pulleys (mm)
D_1	pitch circle diameter of the driving pulley (mm)
D_2	pitch circle diameter of the driven pulley (mm)
N_1	rpm of the motor shaft
N_2	rpm of the solid core

Abbreviation

AFF	abrasive flow finishing
MR	magnetorheological
MRF	magnetorheological finishing
MRAFF	magnetorheological abrasive flow finishing
CIP	carbonyl iron particles
SIC	silicon carbide
MRAH	magnetorheological abrasive honing
RMS	root mean square
CAD	computer aided design

HMI	human machine interface
RPM	rotation per minute
ANSYS	analysis of systems
FEM	finite element method
MRP	magnetorheological polishing
SEM	scanning electronic microscope
PLC	Programmable logic controller

CHAPTER 1

Introduction

1.1 Introduction

Many précised finishing technologies are growing rapidly and have a lot of impact on the development of new products and materials. The traditional finishing processes i.e. grinding, honing etc. are incapable to meet the nano finishing of the materials. Also there are chances of damaging the surfaces using traditional processes. Basically honing is carried out to do the finishing of the internal surfaces of cylinders. But the main problem during the finishing of the surfaces using honing that forces acting on the surfaces cannot be controlled externally. Due to this there are the chances of damage of sub surfaces. Also, the nano level of finishing cannot be achieved by the traditional honing process. The fatigue life of the material will be more affected by the poorer surface finish (Bayoumi *et al*., 1995). Due to which chances of failure of material is high.

1.1.1 Traditional Finishing Processes

The various types of finishing processes such as grinding, lapping, honing etc. are available. Main limitation of the traditional processes is that there is less control over the forces during the finishing processes. This leads to the material failure and likely to poor surface finishing. Different kinds of traditional processes are given below:

1.1.1.1 Grinding

Grinding process is most commonly used finishing process. In case of grinding, the material removal takes place by the relative motion of cylindrical abrasive wheel onto the work material as shown in Figure1.1. During grinding, abrasive particles eliminate the layer of material from the work piece up to the roughness value 1µm. In the grinding process, abrasive particles get frank and chip fill up the gap between the abrasive particles. Due to this

material elimination takes place. The continous re-dressing of the grinding wheel is necessary for providing the finishing of work material.

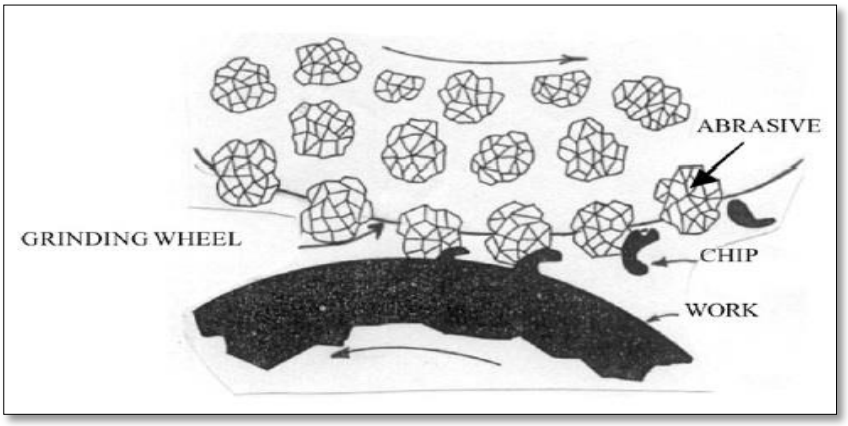

Figure 1.1: Grinding process (Jain, 2012)

The whole process of dressing and truing of grinding wheel is quite expensive, less productive and also very time consuming. Normal force acting in grinding operation is high that leads to the sub surface damage.

1.1.1.2 Laping

Laping process uses the loose abrasives to in order to finish the surface. Lapping is one of the low speed, low pressure operation that results in tremendous accuracy, modification of small imperfections in shape, improvement in surface finish and also exceptionally close fitted structure. The main principle of laping process is the abrasion action by hard particles entrapped between the work materials.

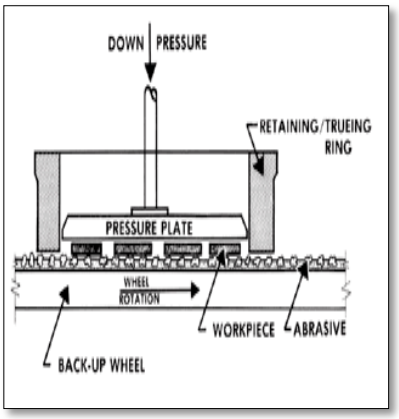

Figure 1.2: Laping process (http://www.columbiagrinding.com/lapping.html)

1.1.1.3 Honing

Honing process is used for metallic as well as non metallic work piece surfaces. This process is used to finish internal surfaces of cylinder. In this process material removal takes place due the reciprocity and rotary motion of the tool (stone). Abrasives are in the form of stones passed through the internal surface of the work material. Reciprocity and rotary motion of the tool is used to generate arbitrary cross-marked surface with fine finish. In honing process a large area of work piece is covered therefore the generation of temperature is low.

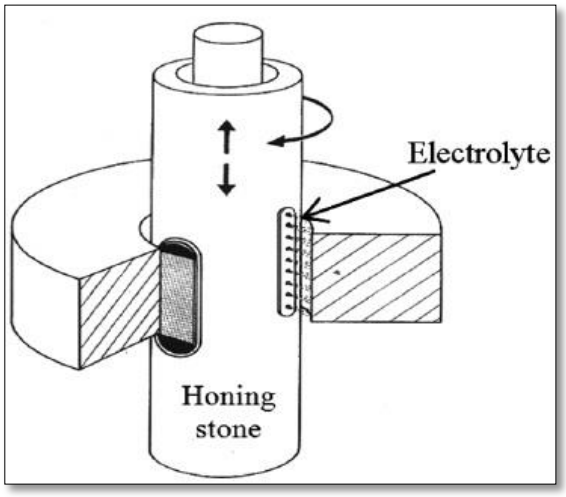

Figure 1.3: Electrolytic honing (Jain, 2012)

Limitation of the honing process is the low finishing rate and also only used for the cylindrical surfaces only.

1.1.2 Advance Finishing Processes

The advanced finishing process is used to finish complex 3D shaped component with a nanometer surface roughness and being most demanding (Jain, 2009). The precise surface accuracy lies in the range of 10-100 nm, whereas for surface roughness is fewer than 10 nm RMS can be achieved with these processes (Zantye *et al*., 2004). In the advance finishing process there is very less sub surface damage as there is less normal forces acting onto workpiece and also it increases the life of the workpiece. Advance finishing processes are suitable for finishing of optical components.

Advanced finishing processes are divided in two categories:

- Without external control of forces.
- With external control of forces.

1.1.2.1 Abrasive flow finishing process (without control of external forces)

Abrasive flow finishing process uses the abrasive particle together with the carrier for a finishing of the wear resistant material. The main components used in the AFF are the machining unit, the tool, different types of abrasives and types of carrier (Rhoades, 1988). The experimental setup consisted of a two vertically opposed piston arrangement for forcing the abrasive particles to and fro through a channel formed by the tool and the workpiece as shown in Figure 1.4. It uses a polymeric carrier in order to get a precise finishing of the component (Uhlmann *et al*., 2013). The axial force component is responsible for the removal of chip, whereas radial force is dependable for the indentation of abrasive onto the workpiece. AFF process is used to improve the performance of elevated speed automotive engines by improving the surface finish of internal passage of intake ports (Lam, 2000).

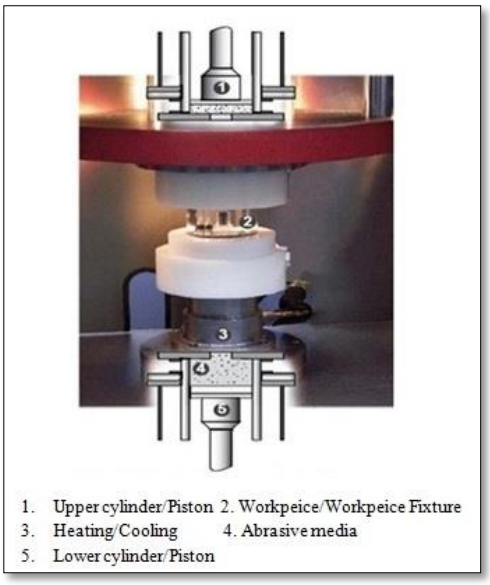

Figure 1.4: Experimental setup of abrasive flow finishing process (Uhlmann *et al.*, 2013)

Shankar *et al.*, (2009) compare the performance of surface finish by using AFF and R-AFF on three types of workpiece namely Al alloy, Al alloy/SiC MMC with 10%SiC and Al alloy/SiC MMC with 15% SiC. The rate of extrusion pressure and the number of cycles remains constant, whereas the workpiece rotational speed varies. The results concluded that R-AFF process can produces 44% better ΔRa and 81.8% of MRR.

1.1.2.2 Elastic emission machining

This process has the capability to remove the material from the workpiece surface at the atomic level by mechanical action and produce the smooth surface.

In this process ultra fine abrasive particle strikes the individual atom and split out from the main surface as shown in Figure 1.5. It has been found that the process of material elimination is a surface energy phenomenon in which every abrasive particle eliminates number of atoms after make contact with the workpiece surface (Mori et. al, 1987).

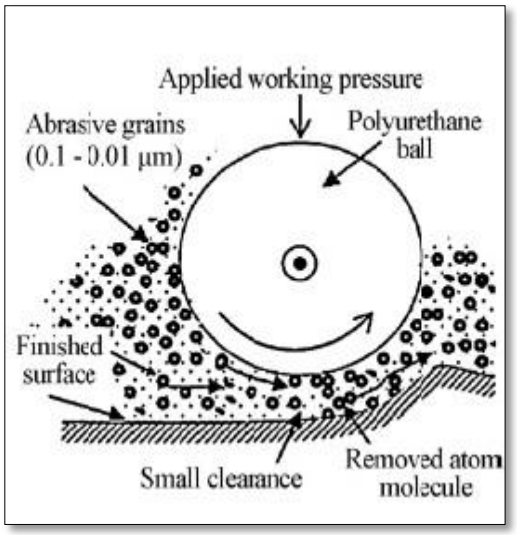

Figure 1.5: Elastic emission machining method (Jain, 2009)

1.1.2.3 Advance finishing process with external control of forces

Advance finishing processes with external control of forces are magnetic field assist finishing processes. In these processes, it is feasible to control the forces acting on the workpiece by changing the DC current passes through the electromagnetic coil or by changing the working gap. A change in the DC current changes the magnetic field in the working area by means of which normal force exert by the abrasive on the workpiece changes (jain, 2009). As the value of normal force changes it can finish the critical part at lower rate so that there is no damage to the surface occurs. Different advance finishing processes with external control of forces are given below:

1.1.2.4 Magnetorheological finishing (MRF)

MRF is magnetic field dependent precise finishing method .MRF is widely used for optical glass and crystals. MRF machine is shown in Figure 1.6.

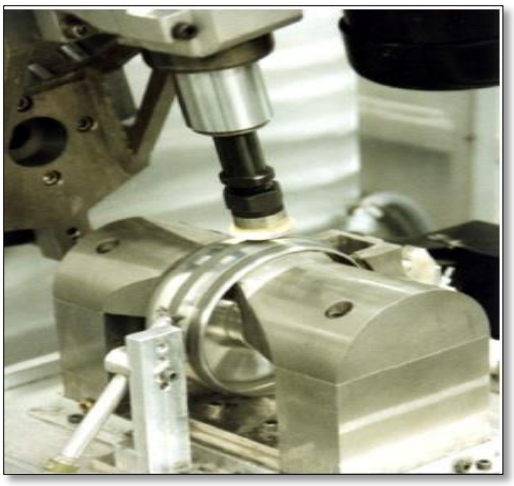

Figure 1.6: Magnetorheological machine (Kordonski *et. al*, 1999)

Magnetorheological fluid consists of a magnetic particle and abrasive particles diffuse in a fluid such as silicone oil, paraffin oil. In the lack of magnetic field the MR fluid exhibit Newtonian behaviour. The effect of magnetorheological behaviour was observed by the function of an external magnetic field to the MR fluid. The particles were randomly distributed due to the absence of an external magnetic field as shown in Figure 1.7 (a). Due to the effect of external magnetic field the CIPs becomes magnetize and form a columnar type arrangement as shown in Figure 1.7 (b).

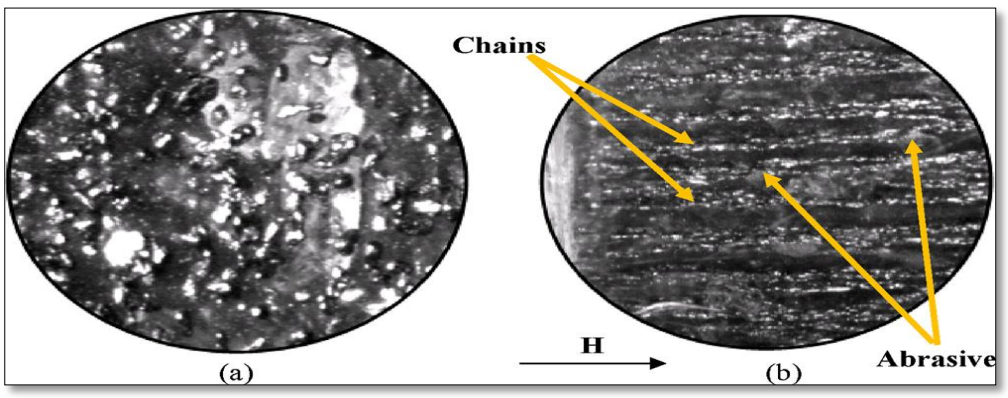

Figure 1.7: (a) MR-Fluid in absence of magnetic field (b) MR-Fluid in presence of magnetic field (Harris, 2011)

In MRF, magnetorheological fluid is deposit by the nozzle on the rim of the rotating wheel as shown in Figure 1.6(a). It demonstrates that abrasive particles are getting in touch with the

workpiece surface and MR fluid is closer to rim of the rotating wheel. The normal force which is usually known as penetrating force transferred to the work material via the abrasive particles and penetrates the workpiece surface. Material removal takes place in the form of chips ensuring nano finishing due to the relative motion between the abrasive particles and the workpiece surface (2009).

1.1.2.5 Magnetorheological abrasive flow finishing (MRAFF)

(Jha and Jain, 2004) developed the magnetorheological abrasive flow finishing process. The limitation of the abrasive flow finishing process is that it is uncontrollable process i.e. the different forces exerted on the work surface cannot be restricted. So to preserve the flexibility of the abrasive flow finishing process a hybrid process termed as MRAFF has been developed (jain, 2009) as shown in Figure1.8.

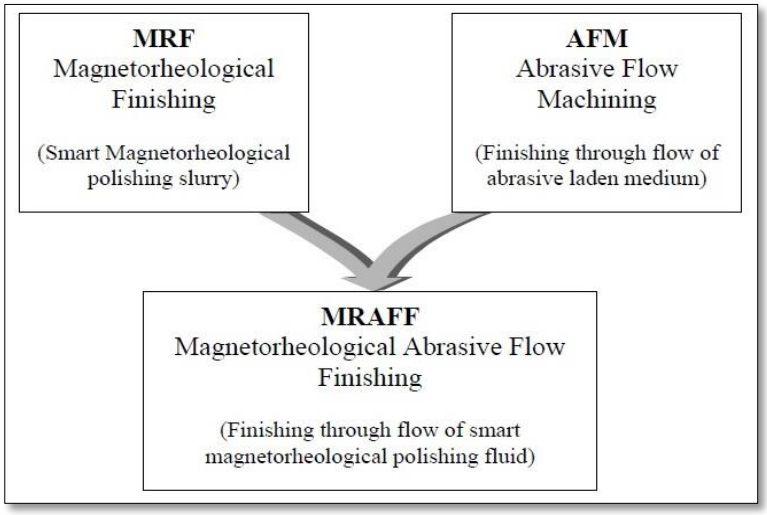

Figure 1.8: Development of MRAFF process (Jha and Jain, 2004)

MRAFF process has the ability to finish the internal and external surfaces up to the nano stage. This process comprises of MRP fluid consist of super fine abrasive particles isolated in it. As the magnetic field applied, CIPs forms the columnar arrangement with abrasive embedded in between the chains. The abrasive particles are held by the CIPs chain graze the workpiece surface and remove the peaks from workpiece surface as shown in Figure1.9.

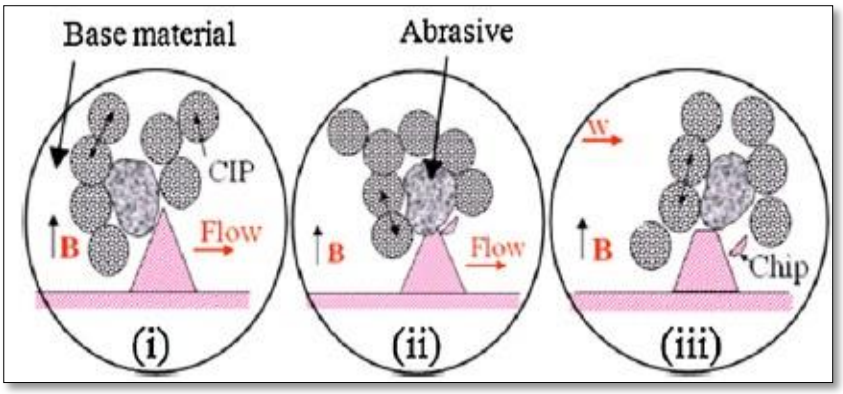

Figure 1.9: Three stage of material elimination in case of MRAFF (Jain, 2009)

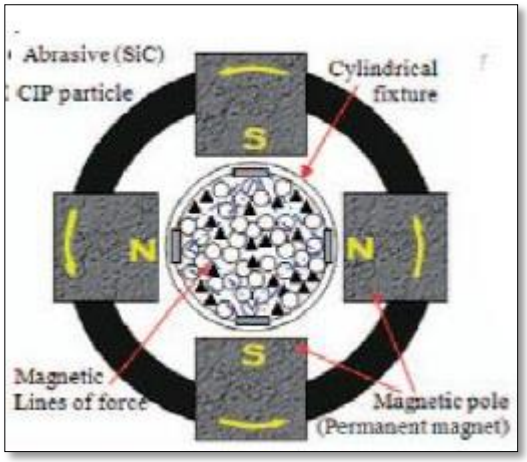

Figure 1.10: Mechanism of MRAFF process (Das *et. al*, 2010)

The amount of material remove from the peak depends upon the bonding strength of CIPs and abrasive particles. The bonding strength can be changed by altering the value of magnetic field applied and the extrusion pressure applied through the piston. That why it is called a controllable process.

1.1.2.6 Magnetorheological jet finishing

The Magnetorheological jet finishing have been newly developed for finishing of parts with a freeform optics, steep concave, cavities etc. This type of finishing process is a modification of MRF process in which MR fluid mix with magnetic abrasive is jetted on the internal surface of the work material and is magnetized on the application of current when MR fluid flows out of the nozzle. The magnetic abrasive particles finish the internal surface of the

work material more precisely. The jet snapshot image of magnetic abrasive jet finishing is as shown in Figure 1.11. The jet of water loses its coherence when passes through the nozzle. When the magnet is off, the jet of MR fluid passes through nozzle losses its coherence due to its high viscosity. When the magnetic is on, the stable jet of MR fluid passes through the nozzle with low viscosity and high velocity jet as shown in Figure 1.11.

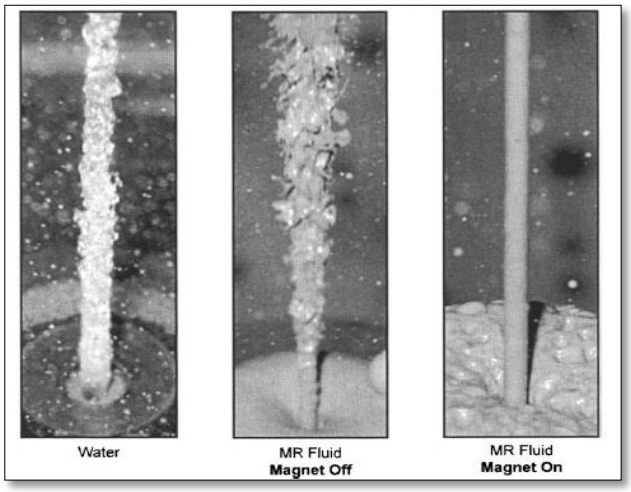

Figure 1.11: Jet snapshot photograph (velocity- 30 m/s) (Kordonski *et al*., 2005)

Kordonski *et al*., (2006) performed their experiment on newly developed magnetorheological jet finishing method for finishing of fused glass silica. The finishing was done by MR fluid (usually mixed with magnetic abrasive particles). The experimentation was performed both on flat and concave shaped work material. The result concluded that the surface roughness of flat and concave shaped work material reduces to 0.013 µm and 0.040 µm.

1.1.2.7 Magnetorheological abrasive honing (MRAH)

Sadiq and Shunmugam (Sadiq and Shunmugam 2009) developed the finishing process known as magnetorheological abrasive honing (MRAH) process. This process is similar to the conventional honing process except the workpiece is given rotation while in conventional honing process the stone (tool) was rotated. The workpiece rotates inside the medium and for the same time reciprocating motion is given to the medium as shown in Figure 1.12. Experimentation was done on stainless steel and aluminum workpiece.

From the experiments researchers are concluded that the surface finishing was improved by increasing the magnetic field density as the fluid develops higher yield strength to shear the peaks from the work surface.

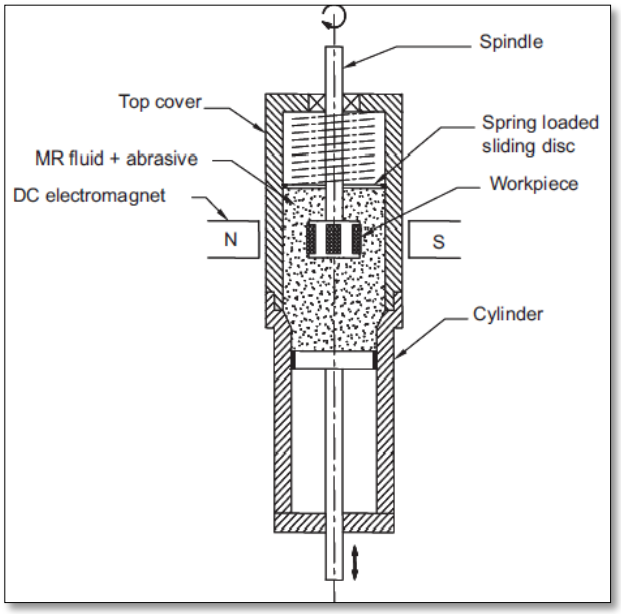

Figure 1.12: Schematic diagram of MRAH process (Sadiq and Shunmugam 2009)

1.1.2.8 Ball end magnetorheological finishing process

MRF and MR jet finishing processes are restricted to particular geometries only such as concave, convex, flat surface due to constraint on relative movement of MRP fluid and workpiece. To overcome this (A. Singh *et al.*) developed a new finishing process for finishing of typical three dimensional surfaces through ball end MR finishing tool as shown in Figure 1.13 (A. Singh *et. al*, 2011) known as ball end magnetorheological finishing process.

In this process the pressurized MR polishing fluid enter from the top of the tool without applying the magnetic field. As soon as MR fluid reaches at the tip of the tool the magnetic field is provided. In this process tool was rotated and the reciprocating motion was provided to the workpiece. The mechanism of ball end type of magnetorheological finishing process is shown in Figure 1.14.

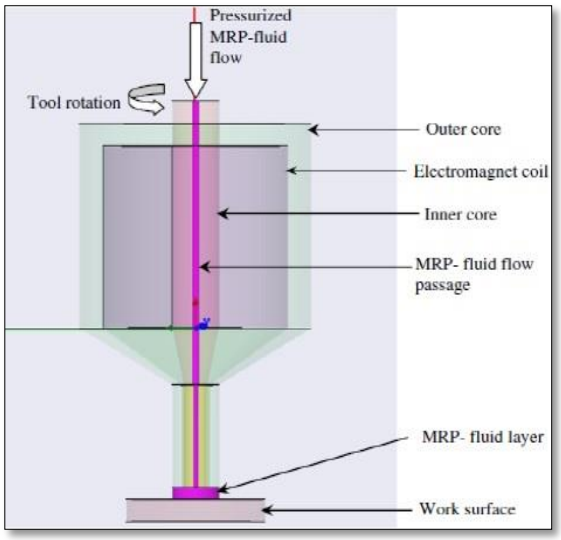

Figure 1.13: Ball end MRF tool (A. Singh *et. al*, 2011)

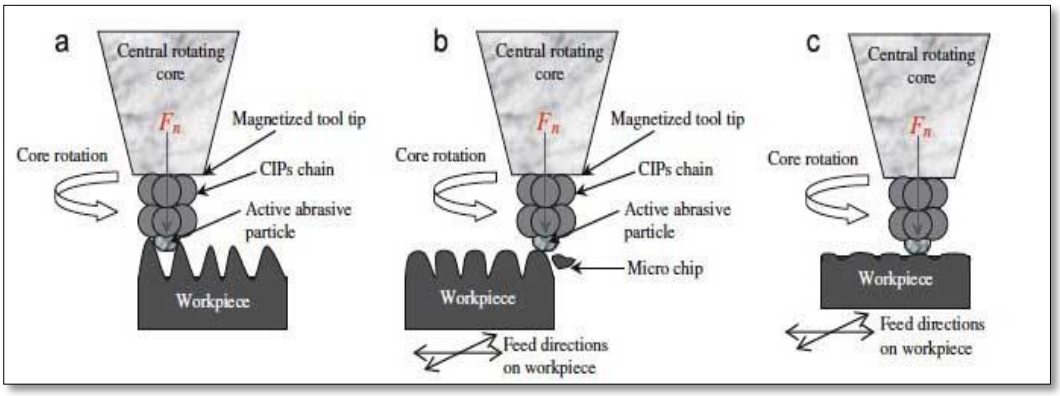

Figure 1.14: Mechanism of ball-end type of magnetorheological finishing process (A. Singh *et al*., 2013)

The material elimination takes place by the action of the shearing stress between the abrasive and work material (Brecker *et al*., 1969). Due to the higher shear strength, the carbonyl iron particles chains will be capable to grasp abrasive particles more tightly. The abrasive particles will penetrate more firmly on the roughness peaks due to higher magnetic field as shown in Figure 1.14 (a). The higher yield strength of MRP fluid rotates on the workpiece surface, than the high shear strength of engrossed abrasives particles will be able to remove the peaks in the form of nano chips as shown in Figure 1.14 (b). When constant feed is provided to the workpiece than the final surface finish can be achieved after wear of roughness peaks due to abrasion as shown in Figure 1.14 (c).

A.Singh *et al*., (2012) performed their experiment in ball-end based MRF tool for finishing of ferromagnetic material (EN31). The finishing was carried out by MR fluid (usually a mixture of 20% CIPs, 20%SiC and 60% Visco plastic base medium. With the process parameters (speed- 500 RPM, current- 4 Amp, time- 30 min and working gap- 0.66 mm), the results concluded that the surface roughness reduces from 142.9 nm to 19.7 nm after 120 min of a time interval.

1.3 Advantages of MR nano-finishing

- Increase part life
- Decrease wear
- Closer tolerances
- High load bearing surface
- No sub surface damage

1.4 Applications of magnetorheological finishing

- Optical industries
- Aerospace and automobile industries
- Medical industries

CHAPTER 2
Literature Review

2.1 Literature review

This chapter provides the literature review of various authors in the field of advanced finishing processes (with/without the help of magnetic properties) and their brief observations are drawn from the authors work and are represented for better understanding.

(Kordonski *et al*, 2004) performed their experiments on newly designed and developed magnetorheological jet finishing process for finishing of fused glass silica (optics). MR jet polishing system was mounted on 5-axis CNC platform equipped with polishing control software developed by QED technology. The MR fluid was prepared with the help of water and abrasives mixture. The initial surface roughness values of fused glass silica were 0.47 µm p-v, 0.14 µm rms. The experimentation was also conducted on small concave fused glass silica with initial surface roughness were 210 nm p-v and 50 nm rms. The roughness profile was measured with the help of (New View 500 white light) interferometer. The theoretical and experimental material removal rate and rate of the work profile was also observed. The results concluded that the surface values of fused glass silica reduces to 13 nm p-v and 2 nm rms whereas, for concave fused glass silica reduces to 44 nm p-v and 6 nm rms.

(Jha and Jain, 2006) performed the experiments on the stainless steel workpiece with different combinations of carbonyl iron particles (CIPs) and the SIC particles. The extent of finishing of the surface depends upon the forces developed on the SIC particles due to the CIPs during the presence of magnetic field. A hydraulic MRAFF experimental setup was developed for the experiments.

Table 2.1: Experimental results of different combinations of CIPs and SIC on finishing value (Jha and Jain, 2006)

Expt. No.	CIP dia. (D_{CIP}) (µm)	SiC dia. (D_{SiC}) (µm)	D_{CIP}/ D_{SiC}	Initial Ra (µm)	Final Ra (µm)	ΔRa^a (µm)	%ΔRa
1.	18.0 (CS)	19.00	0.95	0.32	0.09	-0.23	-17.87
2.	18.0 (CS)	12.67	1.42	0.28	0.17	-0.11	-39.28
3.	18.0 (CS)	7.50	2.40	0.31	0.23	-0.08	-25.80
4.	3.5 (HS)	19.00	0.18	0.26	0.23	-0.03	-11.54
5.	3.5 (HS)	12.67	0.28	0.28	0.24	-0.04	-14.28
6.	3.5 (HS)	7.50	0.47	0.25	0.24	-0.01	-4.00

Best results found in change in roughness value when D_{CIP}/ D_{SiC} kept 0.95. Therefore researchers concluded that magnetic force acting on the carbonyl particle is the function of the particle volume, so the size of the CIPs and SIC affects the roughness value.

(Das *et. al*, 2007) evaluated the effect of current and number of finishing cycles on the surface finishing of stainless steel workpiece using magnetorheological abrasive flow finishing process (MRAFF). The analytical results obtained in the process are validated by the experimental results (Jha et. al, 2004, Jha et. al, 2006). All the experiments were performed at pressure 37.5 bar (Jha et. al, 2004, Jha et. al, 2006). The finishing was done by MR fluid (usually a mixture of 20% CIPs, 20% SiC abrasive powder with 60% visco plastic base medium). The results concluded that with the increase in the number of finishing cycles, the value of surface finish increases in both cases.

(Jha *et al*, 2007) performed their experiment on MRAFF process in order to examine the outcome of extrusion pressure and number of finishing cycles while finishing stainless steel work material. The finishing was carried out with the help of (20% CIPs, 20% SiC abrasive particles and 60% visco plastic base medium. The result concluded that with the increase in extrusion pressure upto 3.75 MPa, and number of finishing cycle, the value of surface roughness improves.

(Cheng *et al.*, 2008) worked on MR fluid for finishing of K9 glass mirror by wheel shaped polishing tool .(usually a mixture of 57.34% silicon oil ,33.84% carbonyl iron powder, 6% cerium agent and 2.82% stabilizing agent). The two sets are conducted for experimental studies (with/without abrasive particles). With viscosity- 8.9 Pa, voltage- 2V, time- 20 min the surface roughness decreases to 0.47 nm.

(Jain, 2009) reviewed the different types of finishing processes such as abrasive based advances micro/nano finishing processes and nano finishing processes with external forces. The author summarizes the work done by the various authors with the help of various finishing processes.

The author concluded after summarizes the work done by different authors that the single slot in the electromagnet during magnetorheological finishing process gives the better surface finishing as compare to no slot in the electromagnet. Also the finishing rate is high in single slotted electromagnet as compare to no slot electromagnet.

(Cheng *et al*, 2010) developed a dual axis MRF tool with internal magnet for finishing of BK7 mirror. The finishing was carried out with the help of MR fluid (includes 10% CeO_2 abrasive particles). The mathematical modelling was carried out in order to calculate material removal. The process parameters were (magnetic field strength- 860KA/m and polishing time- 1 min). The results concluded that the surface roughness value decreases from 328.42 nm to 42.93 nm.

(Sidpara *et al*, 2011) perform the experiments to investigate the forces acting on the workpiece during magnetorheological fluid based finishing process. A dynamometer is used to calculate the tangential and normal forces acting on the workpiece surface by magnetorheological fluid. The parameters selected which influence the normal force and tangential force during the magnetorheological fluid based finishing processes is abrasive particles concentration, wheel speed, CIPs concentration, , working gap. The authors used MR fluid (usually a blend of CIPs and abrasive particle and glycerol).

From the results, it was concluded that the normal force as well as tangential forces decreases with raise in working gap but increases with increase in CIPs concentration. Normal and tangential force rises up to 3.5% concentration of abrasives beyond that value normal and

tangential force starts decreasing. Normal force rises with raise in wheel speed while tangential force rises up to a certain level of wheel rotation after that tangential force starts decreasing working gap is the highest contribution on the forces developed during magnetorheological fluid based finishing.

(Das *et al*, 2012) compare the performance of R-MRAFF with MRAFF in order to study the consequences of extrusion pressure and numbers of cycles on the change in roughness value ΔRa. The finishing was carried out with the help of CIPs, SiC abrasive particles along with visco plastic medium. The preliminary experiment was carried on stainless steel, brass and EN-8 work materials. The result concluded that the highest improvement in surface finish was observed in case of brass whereas least in case of EN-8. The experimental analysis was carried with the help of R-MRAFF for finishing of brass and stainless steel work material by the use of ANOVA method. The process parameters such as rotational speed, extrusion pressure, number of finishing cycles, and vol. Ratio of CIP/SiC were varied. The result concluded that surface roughness of brass reduces to 0.05 µm whereas for stainless steel reduces to 0.11 µm.

(Hong *et al*, 2012) performed their experiment on MR polishing for finishing of alumina reinforced zircon ceramics (3YTZP/Al_2O_3-20%). The finishing was carried out with MR fluid (50% CIPs, abrasive diamond particles and DI water). The main process parameters (speed- 200 and 300 RPM, magnetic field- 3.8, 4.7, 5.5 and 6.1KA/m, Time- 10, 20, 40 and 60 min). The results concluded that with 300 RPM, magnetic field- 3.8 KA/m and electric current- 0.5 Amp the surface roughness decreases from 0.272 µm to 1.960 nm.

(Kang *et al*, 2012) designed and developed a newly built magnetic abrasive finishing (with double dipole tip set) for finishing of austenite 304 stainless steel tube. The mixed type magnetic abrasive consists of (80% iron particles and 20% magnetic abrasive) along with a soluble type barrel finishing compound. The process parameters were (magnetic flux- 1.26-1.29T, speed- 500-30000 rpm, processing time- 10 to 20 min and workpiece pole tip clearance- 0.3 mm). The initial surface roughness of 304 stainless steel was 2-3 µm. The results concluded that at 10000 rpm the surface roughness decrease to 0.1 µm (for 10 min) whereas, the surface roughness at 10000 rpm decrease to 0.11 µm (20 min).

(Judal *et al*, 2013) developed a new vibration dependent magnetic abrasive finishing process for finishing of alumiuium workpiece. The finishing was carried out with the help of steel grit and Al_2O_3 abrasive. The consequences of different process variables such as rotational speed, magnetic flux density and size of abrasive particles on material removal rate were investigated. The result concluded that with the increase in rotation speed and magnetic flux density and frequency of vibration, the value of material removal rate increases. The surface roughness value Ra reduces to 0.18 μm.

(Sidpara and Jain, 2013) studied the angle of curvature of the workpiece surface and rotational speed of the tool with the effect of normal and tangential forces by using magnetorheological finishing process on stainless steel material. The finishing was done by MR fluid (usually a mixture of CIPs, abrasive particles and glycerol). From the results it was concluded that with increases in the angle of curvature ($\theta = 5^o$, 15^o and 25^o) both normal and tangential forces decreases and angle of curvature ($\theta = 5^o$, 15^o and 25^o) increases with the increase in rotations

(Gheisari *et al*, 2014) developed a magnetorheological finishing method for ultra precision finishing of Aluminium work material (cylindrical type). The MR fluid consists of water based suspension of micron sized diamond particles. The process parameters were (current- 9A and working gap- 5 mm). The initial surface roughness of the work material was 170 nm. The experimentation was conducted in three sets. In first set, the work material speed varies from 250-1000 rpm. In second set, the process time varies from 20-100 min. In third case, the effect of a fast RAM on the surface roughness was considered. The results concluded that with the increase in rotational speed (1000 rpm), the surface roughness value improves by 40 nm. With the increase in finishing time (90 min), the value of surface roughness decreases to 42 nm whereas, when the fast RAM (with 0.5 m/sec) was applied, the surface roughness value improves by 78 nm.

2.2 Gaps in literature

From the literature review, a lot of research has been carried out in the field of magnetorheological finishing process. Magnetorheological abrasive honing process is one of the developed process. The following are the drawbacks in the magnetorheological abrasive honing process that are found from literature review.

- The main drawback of the magnetorheological honing process is that it could not do the surface finishing of ferromagnetic surfaces because the magnetic field gradient is low around the tool in the case of ferromagnetic workpiece so it could not finish the ferromagnetic workpiece. Therefore, the magnetorheological abrasive honing process was likely to incapable of finishing the ferromagnetic workpiece surfaces.

- Electromagnet is placed outside the setup therefore the gap between the MRP fluid and the electromagnet is high. Therefore normal force and shear force developed due to magnetic field is low as the working gap is high.

2.3 Objective and methodology

The key objective of the present work is to design and development of magnetorheological honing process. To achieve this main objective the sub objectives are as follows:

-To design and fabricate the honing type tool.
-To design the bracket for holding the tool and motor.
- FEM analysis of the bracket.
- Fabricate the bracket.
- To design and fabricate the flange coupling for coupling the tool holder and the honing tool.
- To design the fixture for fixing the slip ring and carbon bush.
- To design and fabricate the fixture for holding the cylindrical workpiece.
- Synthesis of MRP fluid.
- To demonstrate the process capability for finishing of internal surfaces of ferromagnetic and non ferromagnetic work pieces.

So the current work is to design and developed the magnetorheological honing process. In this chapter a step by step methodology is followed for the process. The important parameters which influence the design are:

- Proper selection of the z- slide.
- Selection of servomotor.
- Design and FEM analysis of bracket for mounting the servomotor and the tool holder shaft.
- Fixture for holding the cylindrical workpiece.
- Selection of bearing for supporting the rotating shaft.

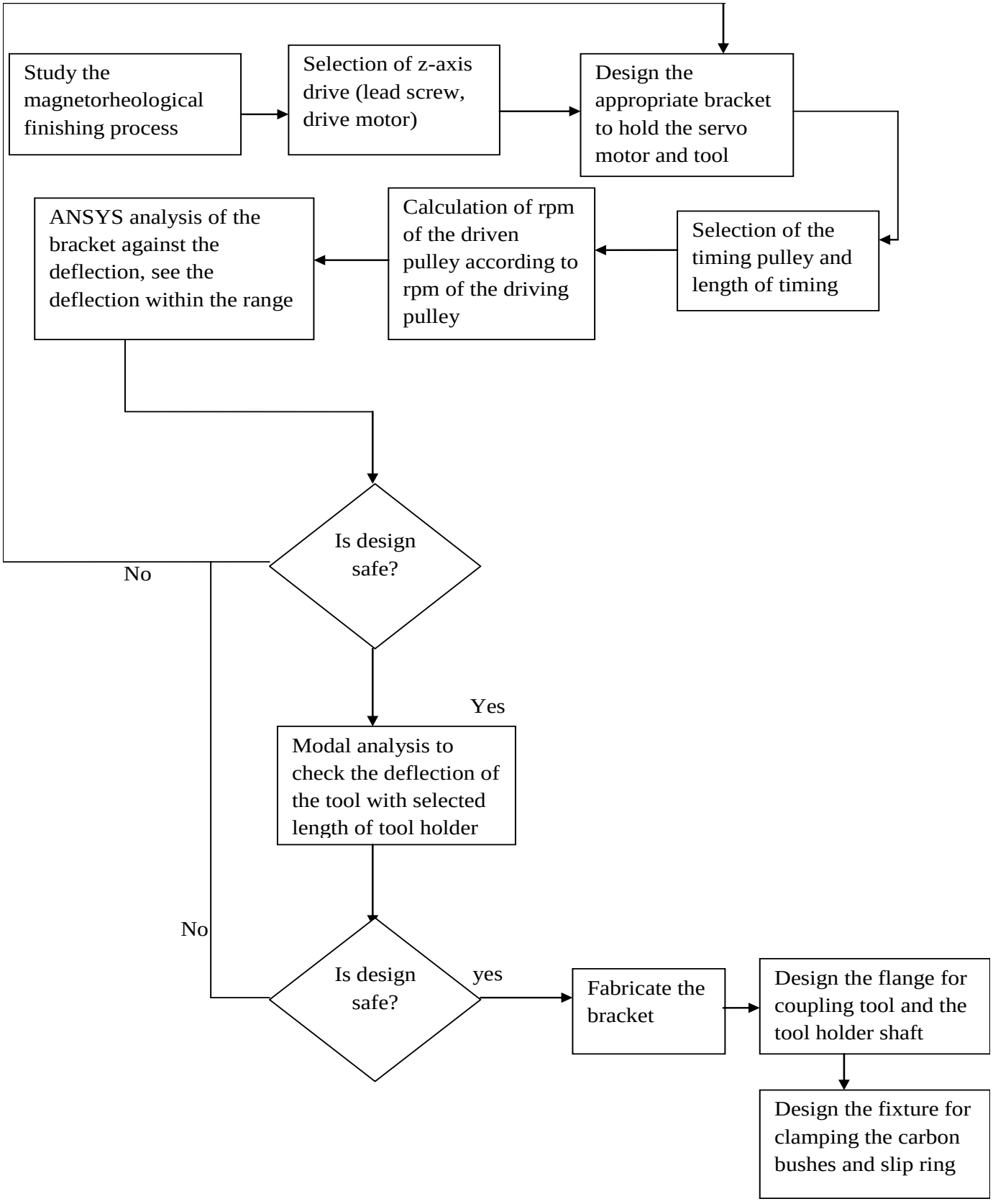

Figure 2.1: Flow chart for the selection process

CHAPTER 3

Design and Development of Magnetorheological Honing Process

Magnetorheological honing process is used for finishing of the internal surface of component. This process is fully automatic. It includes a vertically oriented magnetorheological honing tool which comprises of an I-shaped inner core, electromagnet coil and finishing tool surface. The newly developed magnetorheological honing process is used for finishing of ferromagnetic and non ferromagnetic workpiece.

3.1 Design and development of magnetorheological honing process

The magnetorheological honing tool is the main component of the present developed finishing process as it finishes the workpiece surfaces. The magnetorheological honing tool is positioned on a vertical Z-axis slide. The magnetorheological honing tool is positioned on a vertical Z-axis slide with the help of bracket such that the outer surface of the magnetorheological honing tool can approach on the inner surface of a cylindrical work material and is driven with the help of a servo motor through timing belt and pulleys. The rotational speed of magnetorheological honing tool is precisely controlled with the help of a motion controller. The slip ring, carbon bush and ball bearing are attached on the upper part of magnetorheological honing tool. The cylindrical workpiece is fixed with the help of a precision vice, which is mounted on X-Y linear movement slide. Three servo motors are used for controlling the movement in X-Y-Z directions. The motion controller in X-Y direction is used to control the horizontal movement of cylindrical work material, whereas the motion controller in Z direction is used to control the vertical direction of magnetorheological honing tool. The schematic diagram of the setup magnetorheological honing process is shown in Figure 3.1. CAD model is created for the every part in CREO elements/PROE and after that static structural and modal analysis using WORKBENCH 14.5 is done for the bracket which is used for mounting the servo motor and tool holder shaft. The flow chart described in the Figure 2.1 shows the design step to be followed to reach the fabrication of the bracket. The

knowledge of the machine design, strength of material is considered at each step of selection and calculation.

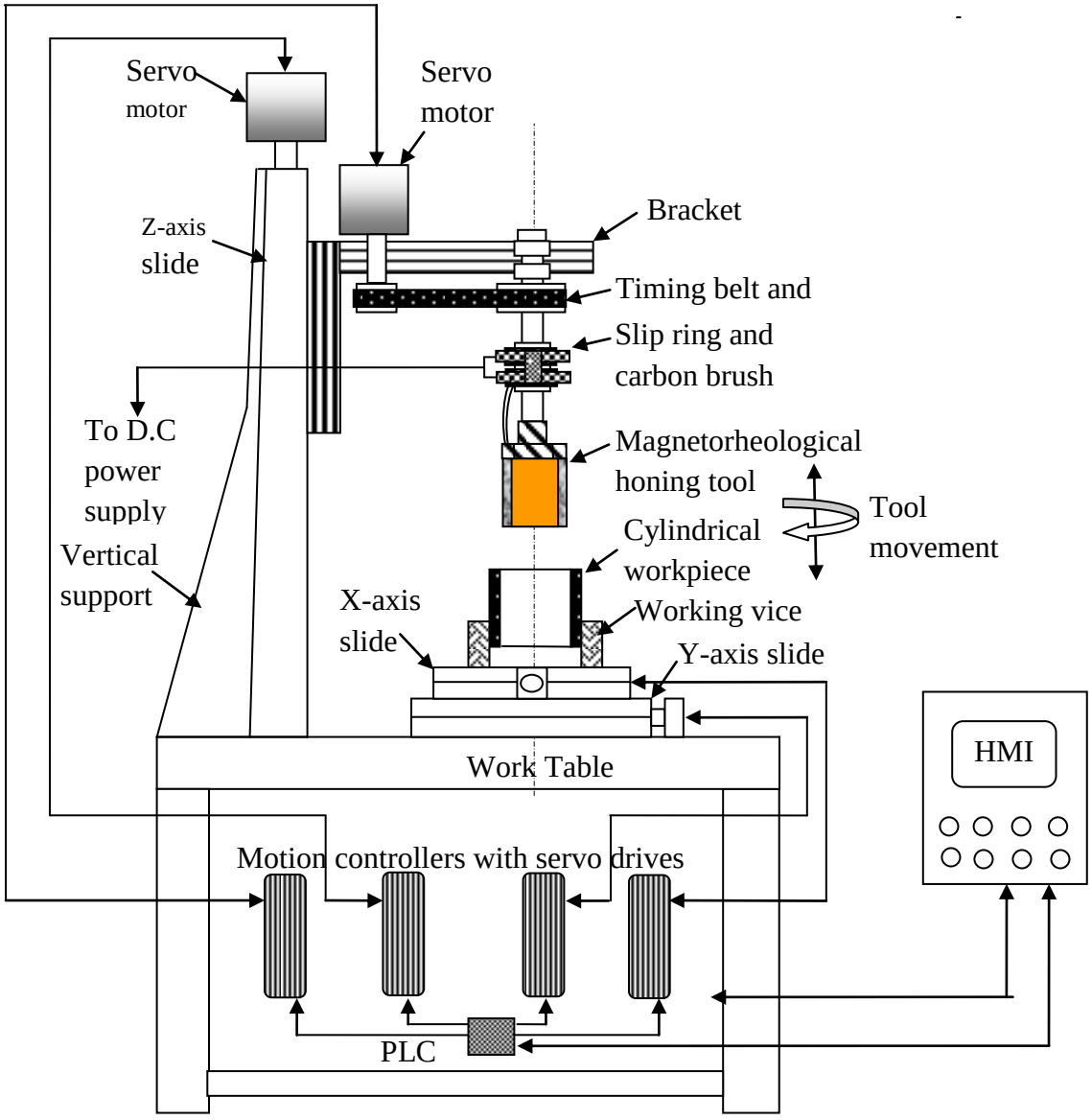

Figure 3.1: Schematic diagram of the setup of magnetorheological honing process

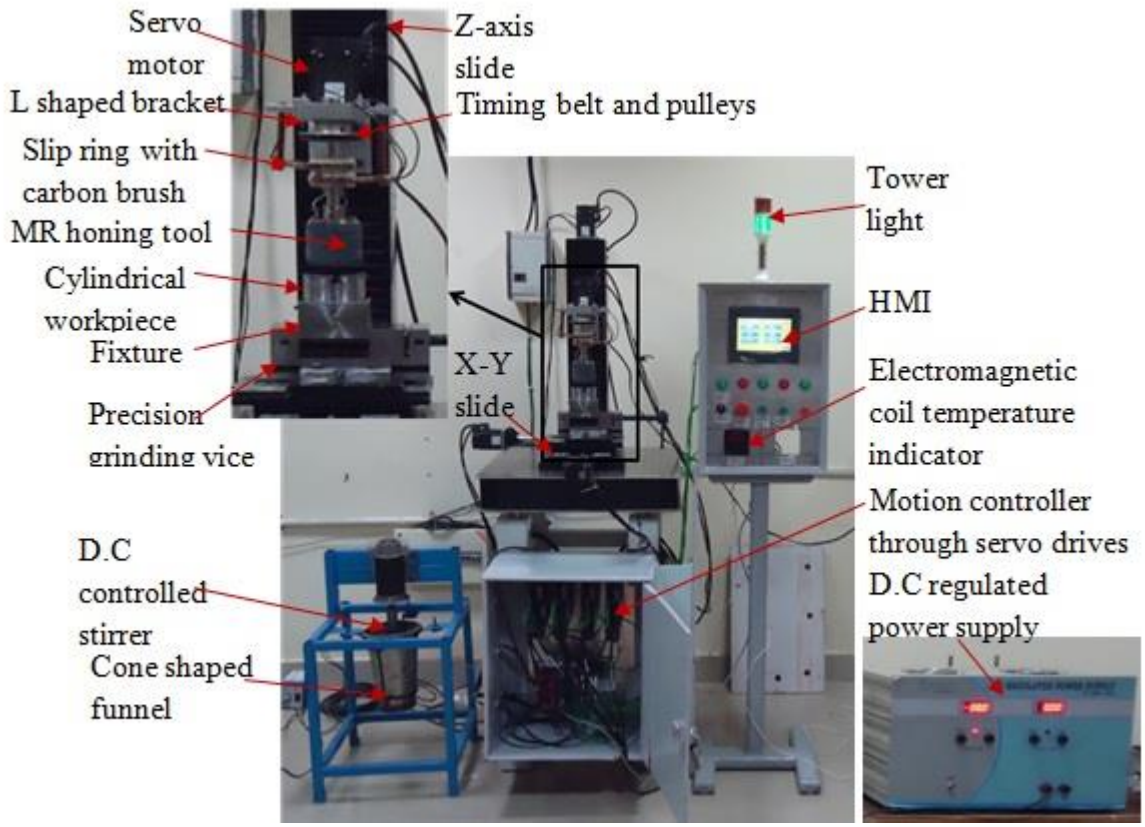

Figure 3.2: Newly developed magnetorheological honing process setup

3.2 Mechanism of material removal

The magnetorheological polishing fluid is applied on the finishing surface of the magnetorheological honing tool so that with the application of magnetic field, the magnetorheological polishing fluid become stiffened at the finishing surface of the tool and finally performs a finishing action. With the increase in magnetic field strength, the magnetic carbonyl iron particles aligned themselves to form a chain like structure over the silicon carbide abrasive particles and hence forms a cutting action. The stiffness of magnetorheological polishing fluid is controlled by means of controlling the magnetizing current induced during finishing. The schematic representation of different forces induced during magnetorheological honing process is shown in Figure 3.3. The bonding strength formed by the magnetic forces between the magnetic particles over the abrasive particle is increased by increasing the magnetic field strength and thereby, results in removing the unwanted peaks from the inner surface of the cylindrical workpiece.

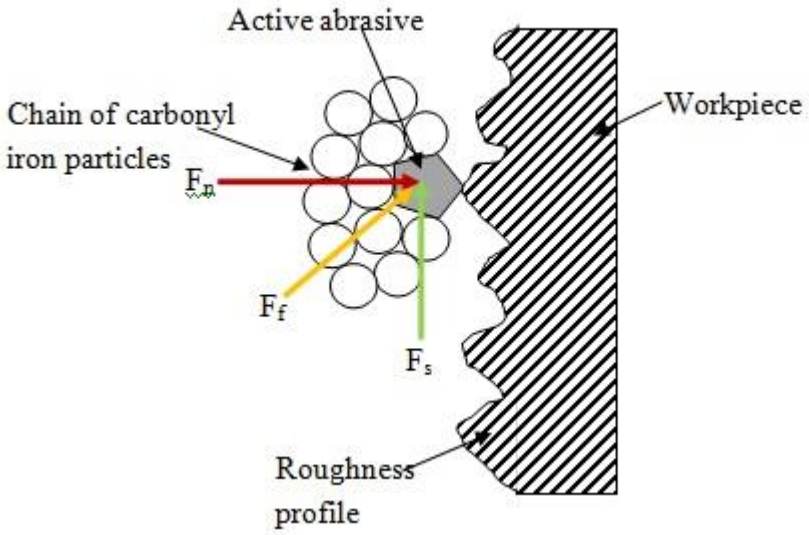

Figure 3.3: Different forces induced during magnetorheological honing process

The finishing mechanism by magnetorheological honing tool with stiffened magnetorheological polishing fluid is shown in Figure 3.4. When no magnetic field is applied across magnetorheological polishing fluid is shown in Figure 3.4(a) i.e. randomly distribution of both magnetic and abrasive particles, as a result no cutting action is performed. When the magnetic field is applied across the magnetorheological polishing fluid is shown in Figure 3.4(b), the carbonyl iron particles surrounds the non magnetic silicon abrasive particles and forms a chain like structure. Hence, the abrasive particles abrade the internal cylindrical surface of work material and perform the cutting action as shown in Figure 3.4(c).

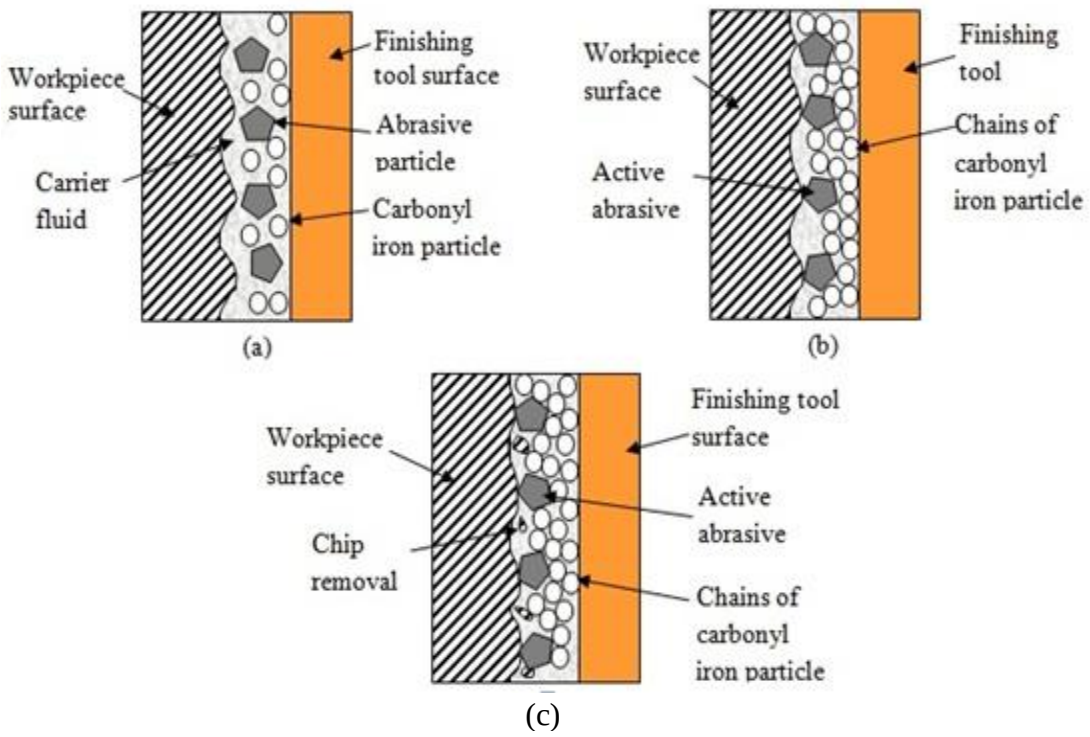

Figure 3.4: Finishing mechanism by magnetorheological honing tool with stiffened magnetorheological polishing fluid

3.3 Magnetorheological honing tool

Magnetorheological honing tool comprises of I shape inner core, electromagnetic copper wire and the finishing surface. Magnetorheological honing tool parameters were decided on the basis of FEA for magnetic flux density distribution. The schematic diagram of the magnetorheological honing tool is shown in the Figure 3.5 and the parameters of the magnetorheological honing tool are shown in Table 3.1.

Table 3.1: Parameters of magnetorheological honing tool

Coil inner diameter	10 mm
Coil outer diameter	68 mm
Total length	40 mm
No. of coil turns	1160

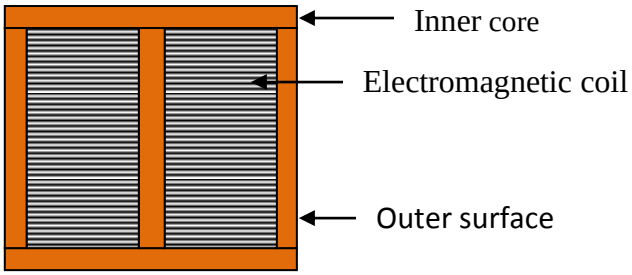

Figure 3.5: Schematic diagram of the magnetorheological honing tool

3.4 Selection of the z-slide

z –slide consist of a lead screw which converts the rotary motion into the linear motion. This is very important step of selection of z-axis slide because the bracket which is used for mounting the servo motor and tool holder is used to attach with the carrier plate of the z- axis slide. The drawing of the z- axis slide is shown in Figure 3.6. The parameters selected for the z- axis slide is shown in Table 3.2.The pitch of the lead screw is 1mm. it means on one complete rotation carriage will move 1 mm. The travelling range of the Z-slide was decided on the basis of height of workpiece because in some cases the height of workpiece is large. So to retain the versatility of the slide moving range was kept 400 mm. The parameters for the selected motor are shown in Table 3.3.The drawing of the selected motor is shown in Table 3.7.

Table 3.2: Parameters of selected z-slide

Pitch of the lead screw	1 mm
Diameter of the lead screw	14 mm
Length of the slide	609 mm
Breadth of the slide	125 mm
Total moving length	400 mm
Material	Aluminum

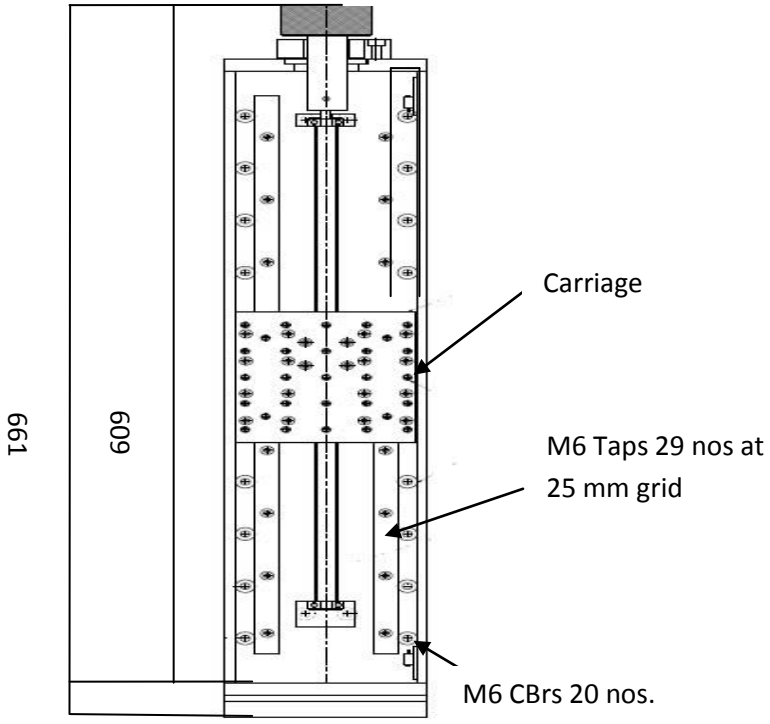

Figure 3.6: Drawing of Z- axis slide

Table 3.3: Parameters of selected drive motor

Weight of the motor	1.4 kg
Power of the motor	400 w
Rpm of the motor	3000 rpm
Maximum torque	4.5 Nm

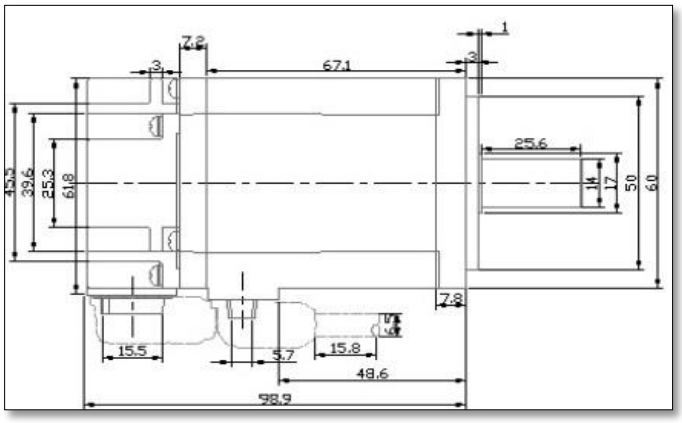

Figure 3.7: Drawing of servo motor

3.5 Designing of bracket

The bracket is required to hold the servo motor and the tool holder shaft. Various designs are considered and analyzed. The material for the bracket is taken as aluminum. The purpose of taken aluminum for bracket was that aluminum posses the non magnetic properties. The CAD model of the bracket is shown in the Figure 3.8 and another model of bracket is shown in Figure 3.9. For the design of bracket consideration taken is:

1. Thickness of bracket.
2. Centre distance between the motor axis and the shaft axis.
3. RPM of the shaft of the tool holder corresponding to the RPM of motor.
4. Length of the shaft.

The material for the shaft is taken as stainless steel as it posses non magnetic properties. Thickness of the bracket and the length of shaft is decided by using FEM analysis in WORKBENCH 14.5 software that will be discussed later.

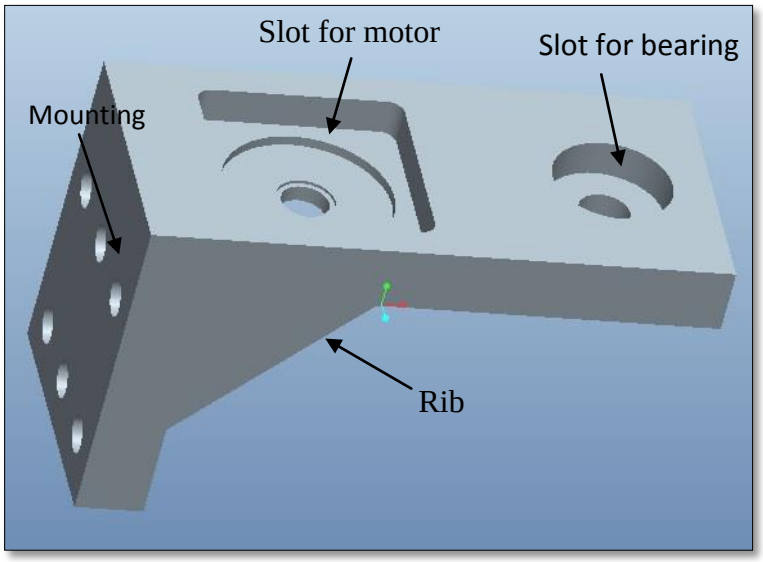

Figure 3.8: CAD model of the bracket (with rib)

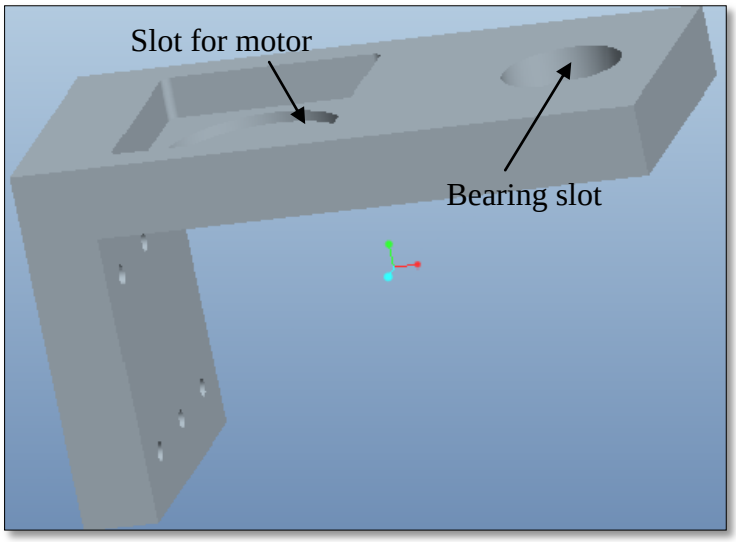

Figure 3.9: CAD model of the bracket (without rib)

3.5.1 FEM analysis of bracket

The design of the bracket is analyzed by FEM analysis in Workbench 14.5 software. The CAD model of the various bracket designs are shown in the Figure 3.8 and the Figure 3.9. Bracket assembly is created in Workbench software as shown in Figure 3.10. Material of the components is as shown in the Table 3.4.

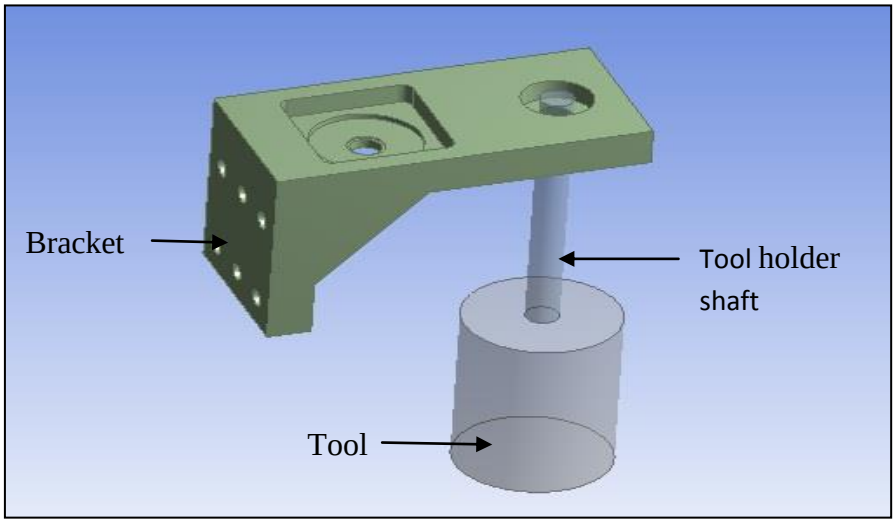

Figure 3.10: CAD model of bracket assembly

Table 3.4: Material of the components for the analysis of thickness of bracket

Component	Material
Bracket	Aluminum
Shaft	Stainless steel
Tool	Soft iron

The mechanical properties of the selected material are shown in Table 3.5, 3.6 and 3.7.

Table 3.5: Mechanical properties of aluminum

Density	2700 kg/m^3
Young's modulus	68.9 GPa
Ultimate tensile strength	241 MPa
Ultimate yield strength	145 MPa
Ultimate bearing strength	228 MPa
Poission's ratio	0.33

Table 3.6: Mechanical properties of stainless steel

Density	7750 kg/m^3
Young's Modulus	193 GPa
Poission's ratio	0.31
Ultimate tensile strength	586MPa
ultimate yield strength	207 MPa

Table 3.7: Mechanical properties of soft iron

Density	7874 kg/m^3
Young's modulus	211 GPa
Poission's ratio	0.29
Ultimate yield strength	90 MPa
Ultimate tensile strength	350 MPa

Hexahedral and tetrahedral mesh was generated with number of nodes 107805 and 68042 number of elements as shown in Figure 3.11.

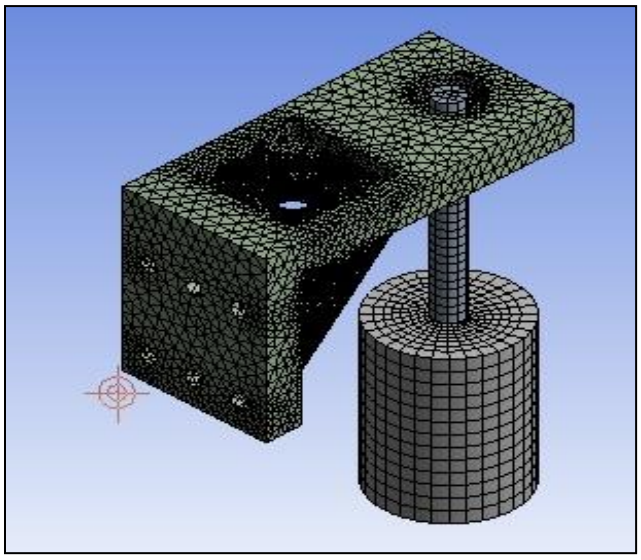

Figure 3.11: Mesh generation in bracket

The initial boundary condition of the bracket assembly is shown in the Figure 3.12. The fixed support is applied to the face that is used to be attached at z- axis slide shown by symbol C and the cylindrical support is applied where bolt is used to attach the bracket with z- axis slide is shown by symbol D. Standard earth gravity is applied for considering the self weight of the bracket assembly is shown by symbol B. Rotational velocity is given to the tool holder shaft as shown in Figure 3.12 by symbol A. Motor weight is given by the remote force shown by the symbol E. revolute joint is given to the tool holder shaft in the z-direction as the tool holder shaft is rotating component. The thickness of the bracket is kept 20 mm and the length of shaft is kept 165 mm. Revolute joint is given the z- direction as shown in Figure 3.13 as the tool holder shaft is rotary.

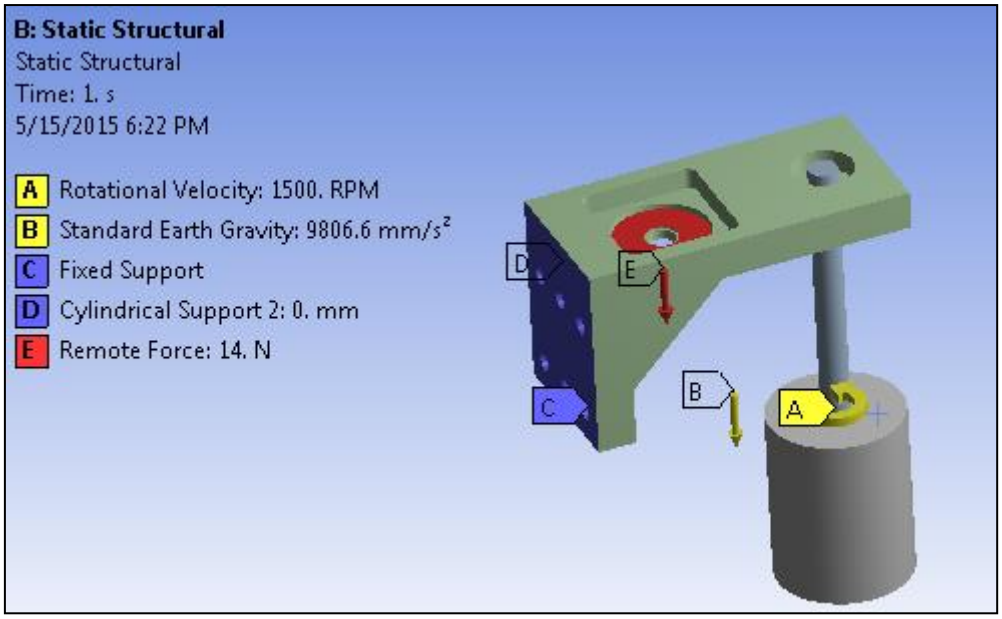

Figure 3.12: Initial boundary condition applied on bracket assembly

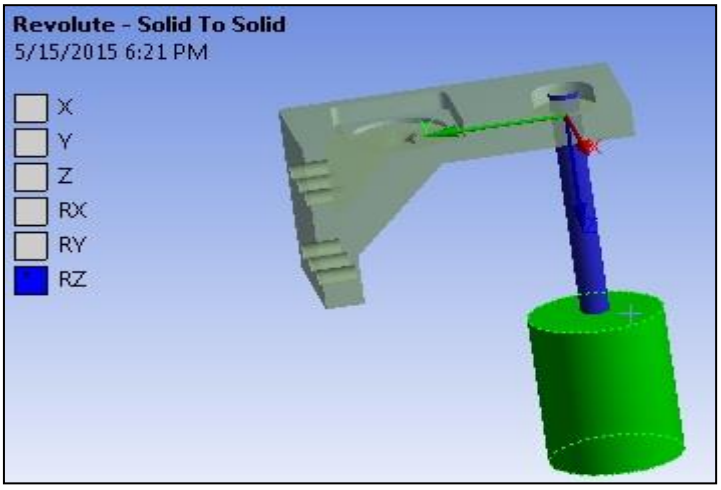

Figure 3.13: Revolute joint

3.5.1.1 Static structural analysis

Structural analysis was performed to obtain stress (von-misses) and total deformation of bracket when the initial boundary conditions applied on it. It is linear analysis type that is performed in static structural analysis. The following results were obtained using this type of analysis shown in Figure 3.14 and 3.15.

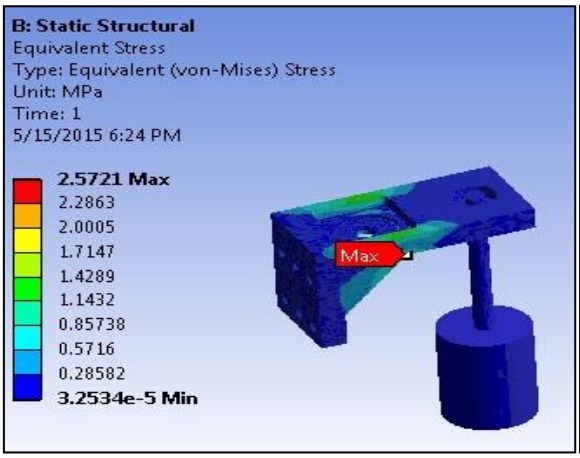

Figure 3.14: Von misses stress

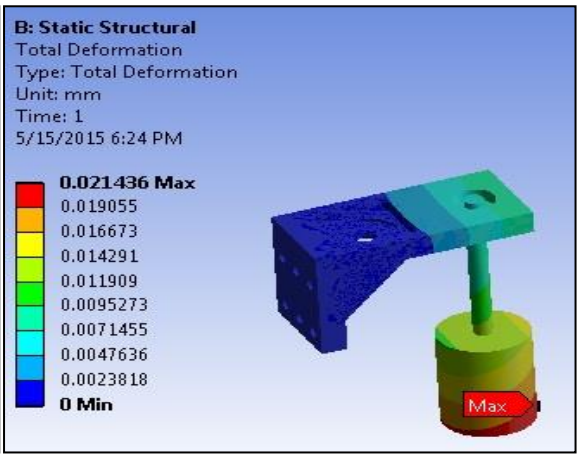

Figure 3.15: Total deformation

From the iteration it was observed that the design is safe in term of deformation. The maximum deformation is shown in Figure 3.15. The value of the stress acting on the bracket assembly is shown in the Figure 3.14. The ultimate yield strength of the aluminum is 145 MPa and the maximum stress acting on the bracket is 2.5721 MPa. So the factor of safety is very high. Therefore the design is ultra safe under the static condition

.

3.5.1.2 Modal analysis of bracket

Modal analysis is used to obtain the different mode shape under the initial boundary conditions as shown in Figure 3.12. The different natural frequencies at different mode shape are given as follows.

Table 3.8: Frequency at different mode shapes

Mode	Frequency (Hz)
1	65.1
2	82.562
3	332.87
4	1239.4
5	1893.6
6	4026.8

Different mode shapes at different frequencies are shown in Figure 3.16.

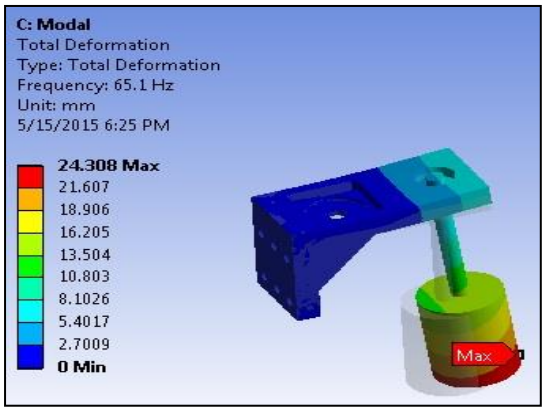

Mode shape 1

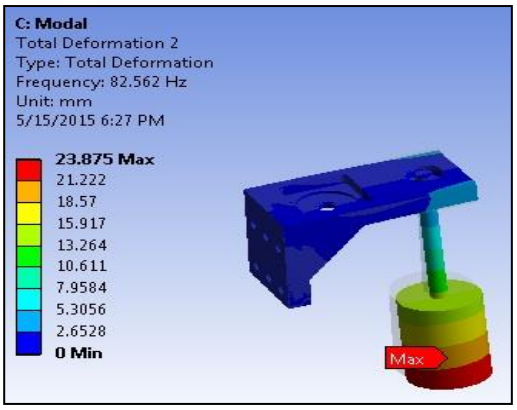

Mode shape 2

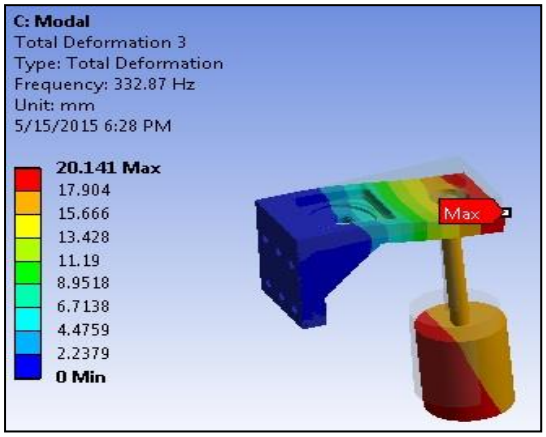

Mode shape 3

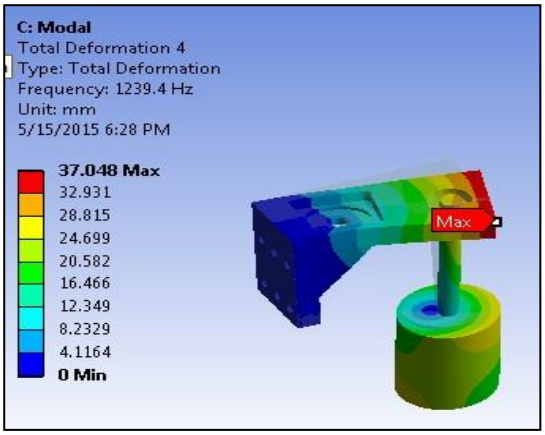

Mode shape 4

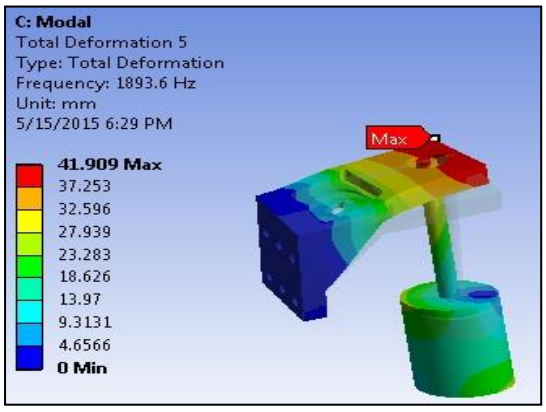

Mode shape 5

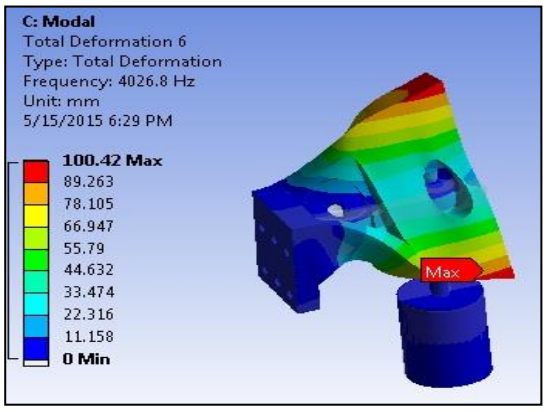

Mode shape 6

Figure 3.16: Different mode shapes of bracket at different frequencies

The natural frequency of the bracket comes out from prestress (static structural) modal analysis is 65.1 Hz. Natural frequency of the bracket assembly is calculated by the rpm/ 60. The maximum rpm of the tool holder shaft is 1500. Therefore the natural frequency of the bracket assembly is 25 Hz which does not match with the frequency calculated in modal analysis. So the design is safe.

3.5.2 Static structural analysis of bracket (without rib)

The design of the bracket assembly is shown in the Figure 3.17. Hexahedral and tetrahedral mesh was generated with number of nodes 105041 and 68042 number of elements.

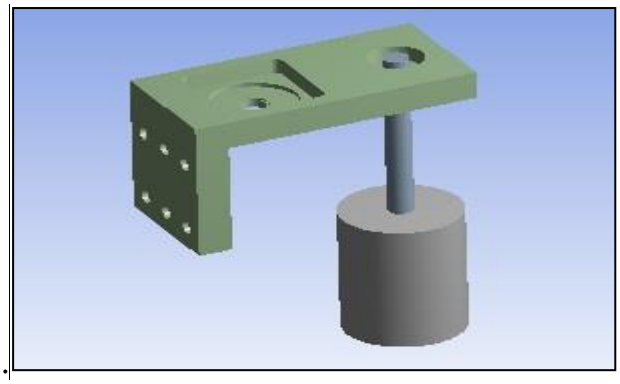

Figure 3.17: CAD model of bracket (without rib) assembly

Under the same boundary conditions as shown in the Figure 3.12 the von-misses stresses and deformation are shown in the Figure 3.18and 3.19.

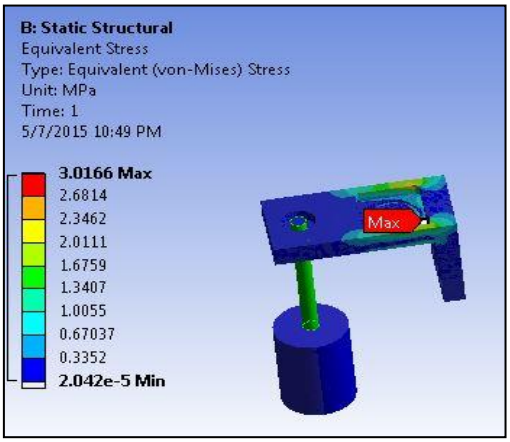

Figure 3.18: Von misses stress

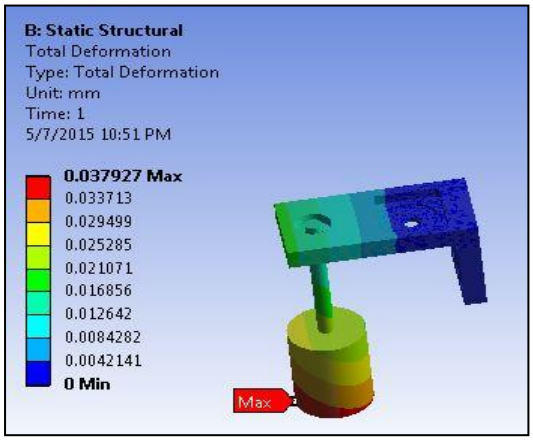

Figure 3.19: Total deformation

From the iteration it was observed that the design is safe in term of deformation. Value of the maximum stress is 3.0166 MPa. The ultimate yield strength of the aluminum is 55.2 MPa and the maximum stress acting on the bracket is 3.0166 MPa. So the factor of safety is very high. Therefore the design is ultra safe under the static condition.

3.5.2.1 Modal analysis of bracket (without rib)

Modal analysis is used to obtain the different mode shape under the initial boundary conditions as shown in Figure 3.12. The different natural frequencies at different mode shape are given as follows:

Table 3.9: Frequency at different mode shapes

Mode	Frequency (Hz)
1	54.846
2	66.86
3	261.79
4	1146.3
5	1765
6	3484.4

Different mode shapes at different frequencies are shown in Figure 3.20.

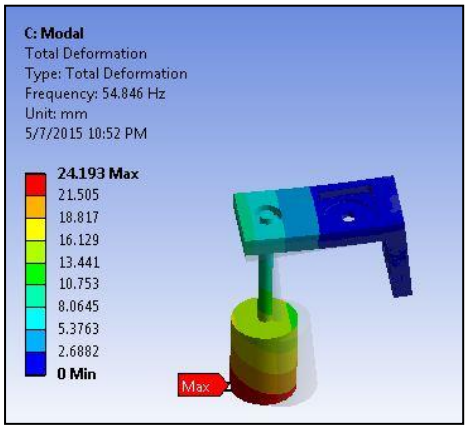

Mode shape 1

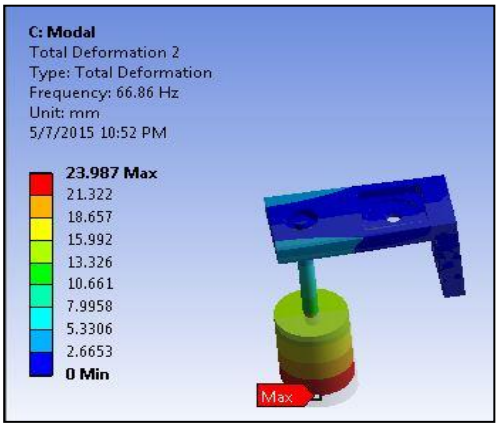

Mode shape 2

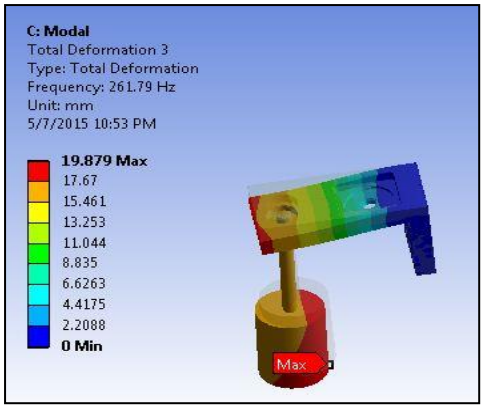

Mode shape 3

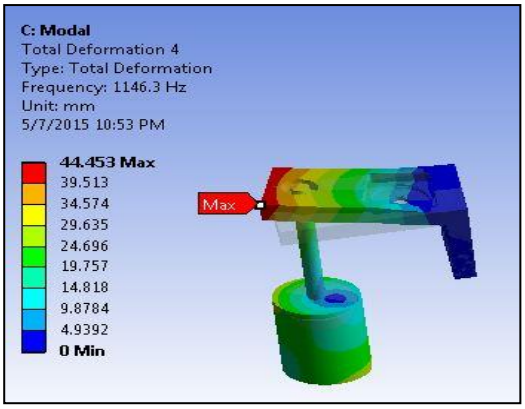

Mode shape 4

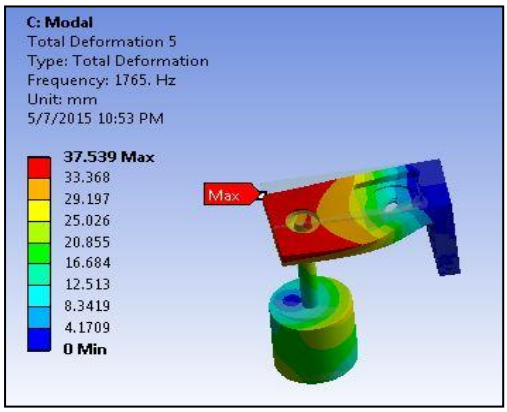

Mode shape 5

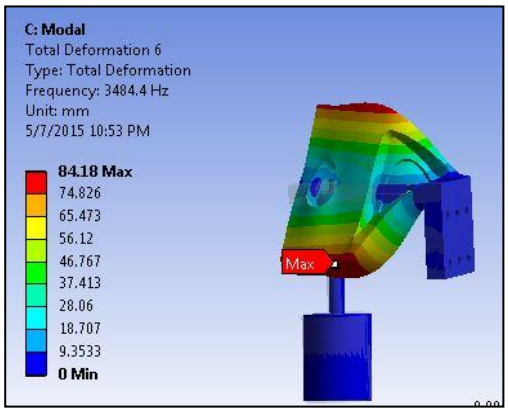

Mode shape 6

Figure 3.20: Different mode shapes of bracket at different frequencies

The natural frequency of the bracket comes out from prestress (static structural) modal analysis is 54.846 Hz. Natural frequency of the bracket assembly is calculated by the rpm/ 60. The maximum rpm of the tool holder shaft is 1500. Therefore the natural frequency of the bracket assembly is 25 Hz which does not match with the frequency calculated in modal analysis. So the design is safe. As the design of the bracket with thickness 20 mm and tool holder shaft length 140 mm with 15 mm diameter is safe therefore fabricate the bracket. The drawing of the fabricated bracket is shown in Figure 3.21.

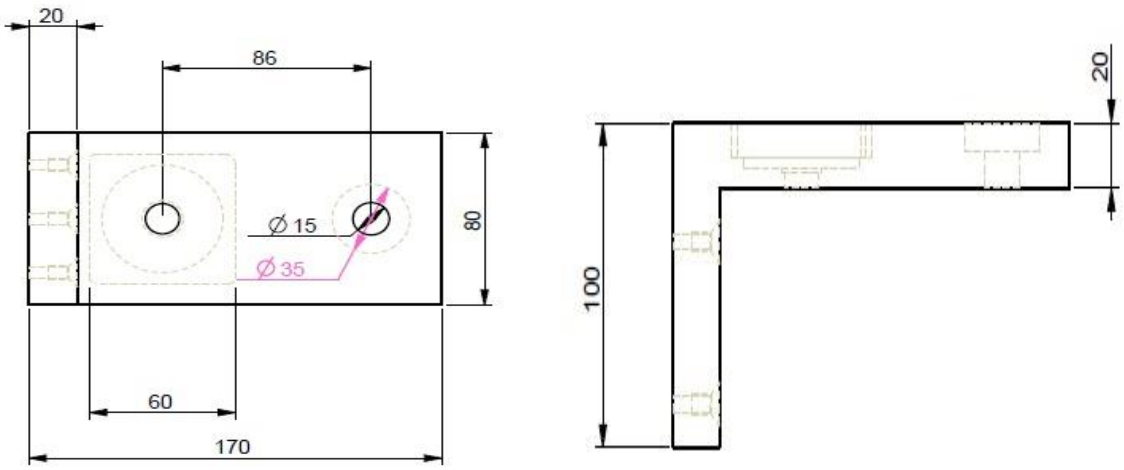

Top view **Front view**

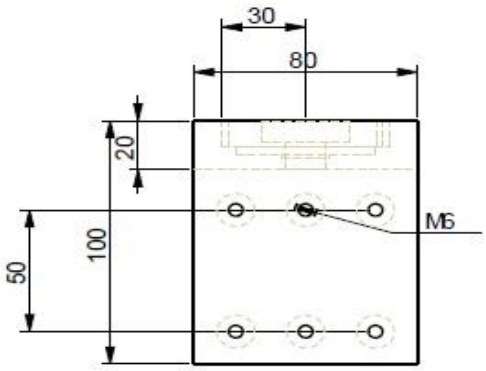

Side view

Figure 3.21: Drawing of the fabricated bracket

3.6 Selection of the timing pulleys

The belt pulley mechanism is used for rotating the tool. Therefore two timing pulleys are selected. One is driving pulley which is attached with the shaft of motor and another pulley is driven pulley which is attached with the tool holder shaft. There are the several reasons for selection of timing pulleys and belt. These are given below:

- Higher speed and power capacities.
- High drive ratio at shorter distance.
- Minimal vibration.
- Synchronization is easy.

- No slippage.
- High mechanical efficiency.

Both pulleys are made up of aluminum. The no. of teeth of the driving pulley is 24 while the number of teeth of driven pulley is 48.

3.6.1 Calculation of the length of belt

Length of belt is calculated by the formulae:

$$L= 2C+\pi(D_1+D_2)/2+(D_1+D_2)^2/4C \qquad (\text{Eq. } 3.1)$$

L= Length of the belt

C= centre distance between the two pulleys

D_1= Pitch circle diameter of the driving pulley

D_2= Pitch circle diameter of the driven pulley

C= 86 mm

D_1= 39 mm

D_2 = 78 mm

By putting the values of C, D_1, D_2 equation 3.1, got the length of belt which is 359.2 mm.

Therefore the timing belt selected for the belt pulley mechanism is 142 XL which is having length 360 mm.

3.7 Calculation of the rpm of the tool holder shaft according to the motor shaft

The rpm of the tool holder shaft according to the motor shaft is calculated by the formulae:

$$N_1/N_2 = D_1/D_2 \qquad (\text{Eq. } 3.2)$$

N_1 = rpm of the motor shaft

N_2 = rpm of the tool holder shaft

D_1 = Diameter of the driving pulley

D_2 = Diameter of the driven pulley

N_1 = 3000 (maximum rpm of the motor)

D_1= 39mm

D_2= 78 mm

Therefore by putting these values in equation 3.2, got the maximum rpm of the tool holder shaft, which is 1500 rpm.

3.8 Design the flange for coupling the tool and the tool holder shaft

Flange coupling is used to couple the tool holder shaft and the magnetorheological honing tool. The magnetorheological honing tool is attached to the flange through the nut bolt arrangement. Flange is made up of the stainless steel. CAD model of the flange is shown in Figure 3.22.

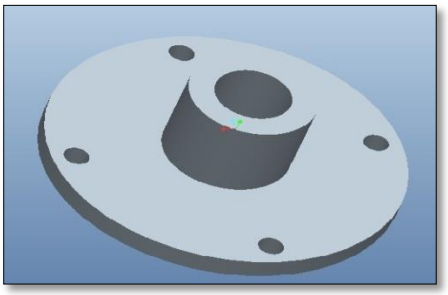

Figure 3.22: CAD model of the flange coupling

The drawing of the flange is shown in the Figure 3.23.

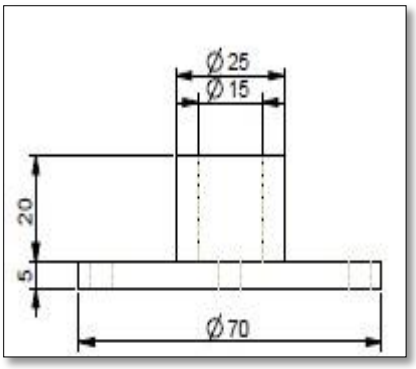

Figure 3.23: Drawing of the flange

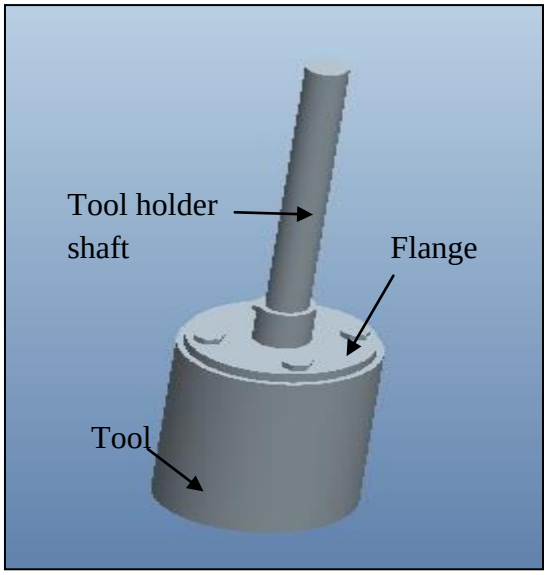

Figure 3.24: Coupling arrangement of the tool holder shaft and the tool

3.9 Carbon bush and slip ring arrangement

Slip ring and carbon bush are used to transmit the power through the power supply to the rotating body. In the magnetorheological honing process tool is rotating. So there is need of the carbon bush and slip ring. To fix the carbon bushes C shape clamping is designed and fabricated. C shape clamping is made up of aluminum. C shape clamping is shown in the Figure 3.25. C shape clamps are fixed to the bracket and tighten with the L- key screw. Slip ring is fitted into the tool holder shaft. The whole arrangement of the slip ring and the carbon bushes is shown in the Figure 3.26.

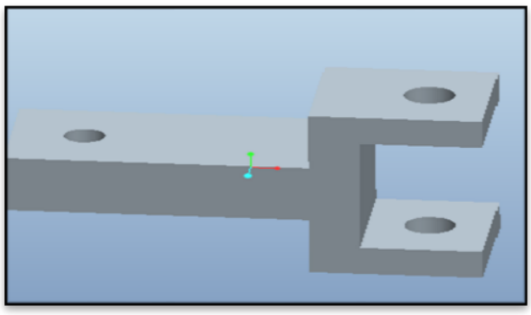

Figure 3.25: C shape clamp for fixing the carbon bushes

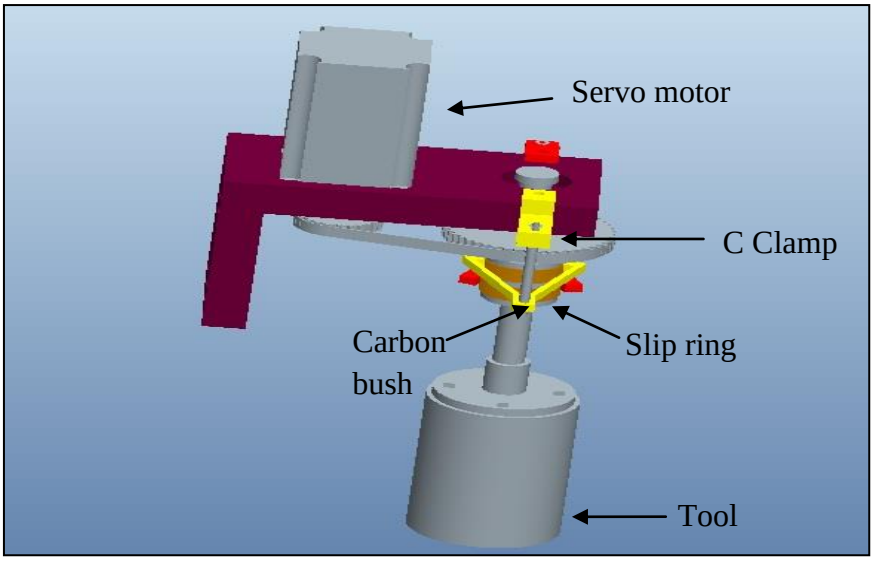

Figure 3.26: Slip ring and carbon bush arrangement

3.10 Selection of bearing

As the internal diameter of the tool holder shaft is kept 15 mm. so the bearing is selected with internal diameter 15mm. there are two categories of the bearing with 15 mm internal diameter as shown in Table 3.10.

Table 3.10: Categories of bearing with internal diameter 15 mm

Internal diameter	Outer diameter	Height
15 mm	32 mm	9 mm
15 mm	35 mm	11 mm

Bearing is selected with internal diameter 15 mm, outer diameter 35 mm and height if 11 mm.

3.11 Fixture for holding the cylindrical workpiece

Cylindrical workpiece is to be fixed into the precision grinding vice with the help of the supporting fixture. The supporting fixture is made up of the mild steel. The drawing of the supporting fixture is shown in the Figure 3.27 and CAD model of the supporting fixture with workpiece is shown Figure 3.28.

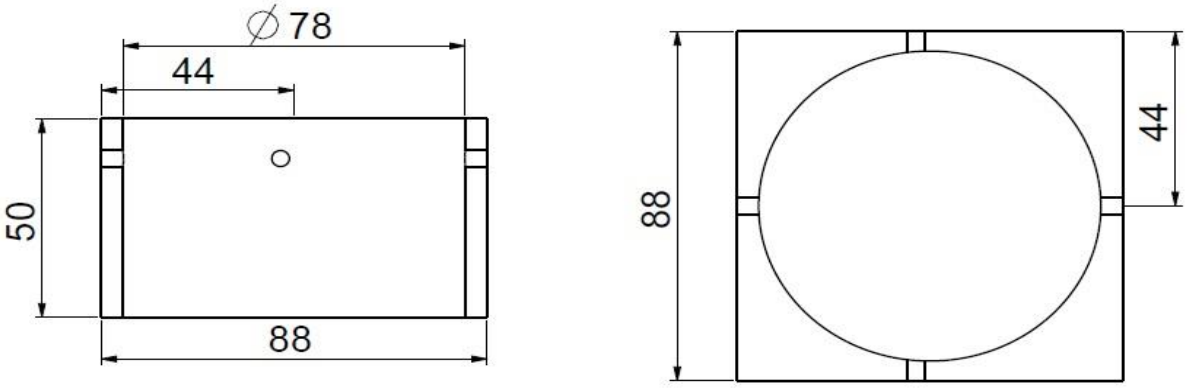

Figure 3.27: Drawing of the supporting fixture

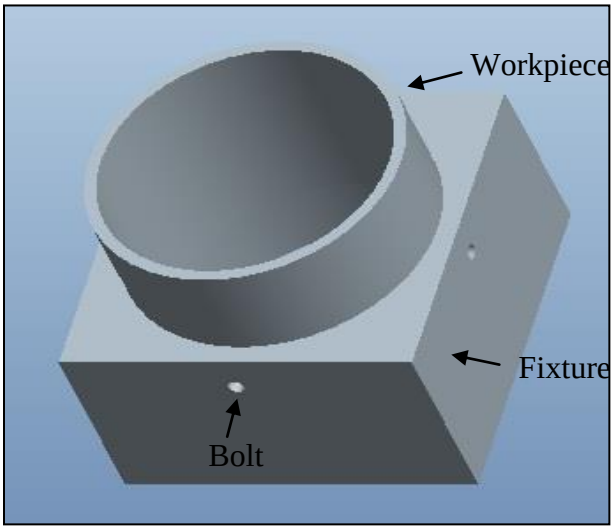

Figure 3.28: CAD model of the supporting fixture

From the FEM analysis that was done in the Workbench 14.5 software it is concluded that the design of bracket assembly is safe in both static and modal analysis under the initial boundary conditions.

CHAPTER 4

Synthesis of MRP fluid and Experimentations

The preliminary experimentation was carried out in order to determine the effect of magnetic field strength (B) and finishing time (t) on both ferromagnetic and non-ferromagnetic workpiece.

4.1 Preparation of MRP fluid

The required magnetorheological polishing fluid had been prepared as per the condition and procedure reported by the authors (Singh et al. 2011) as shown in Table 4.1 and 4.2. Initially base fluid was prepared with mixing of heavy paraffin oil with AP3 grease in a mixing funnel which is made up of stainless steel and multiple blade stirrers with rpm controller on DC motor. Composition of base fluid is shown in Table 4.1. Density of base fluid was found to be 0.76 gm/cm^3 by taking mass and the volume of the base fluid as 15.33 gm and 20ml (or 20cm^3).

Table 4.1 Composition of base fluid

Base fluid	% age by weight
Heavy paraffin liquid	80
AP3 grease	20

After the preparation of base fluid MRP fluid was prepared. Composition of synthesized MRP fluid is shown in Table 4.2.

Table 4.2 Composition of synthesized MRP fluid

Constituents	% age vol. concentration
Carbonyl iron powder	20
Silicon carbide abrasive (800 mesh size)	20
Base fluid	60

Volume of MRP fluid prepared was 400 cm^3. In which, the CIP is 20% by volume =80 cm^3 and by weight= 80 cm^3×7.8 gm/cm^3 (density of CIP) =624 gm=0.624 kg. The silicon carbide

abrasive powder is 20% by volume=80 cm^3 and by weight=80 cm^3×3.22 gm/cm^3 (density of silicon carbide abrasive powder) =257.6 gm. The base fluid is 60% by volume=400 cm^3×60%=240 cm^3 and by weight=240 cm^3×0.76 gm/cm^3 (density of base fluid) = 182.4 gm. These three components of MRP-fluid in above mentioned proportion was mixed and stirred in funnel.

4.1.1 Rheological characterization of synthesized MRP fluid

Rheological behavior of the prepared MRP fluid was carried out by the parallel plate type rheometer known as Anton Paar modular compact rheometer (MCR 301). The gap between the two plates was maintained 1 mm during the rheological experimentation study. Current varies from 0 to 4 ampere. The graph of the viscosity versus shear stress is shown in Figure 4.1 at different value of magnetizing current.

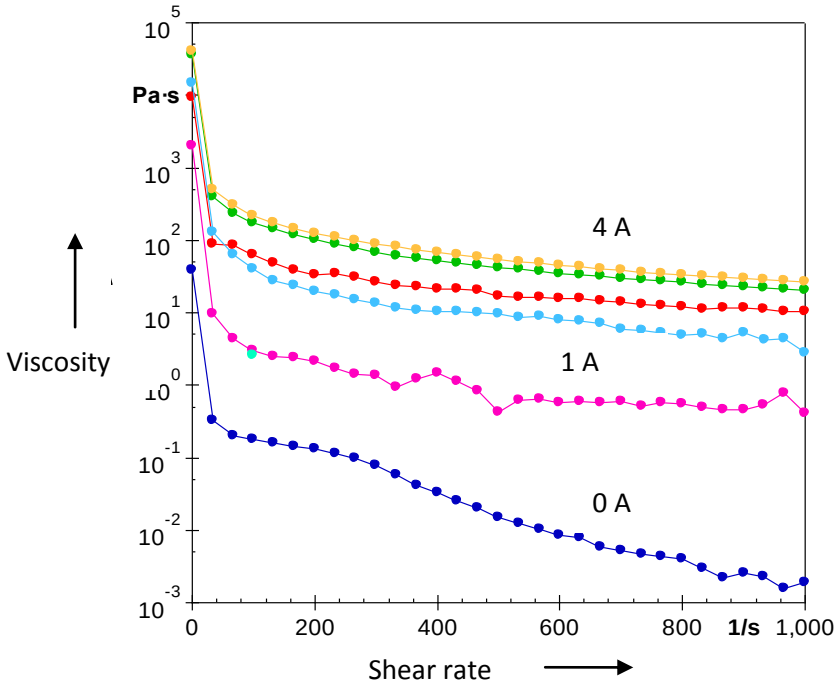

Figure 4.1: Viscosity vs Shear rate

From Figure 4.1 it is concluded that the viscosity increases as the magnetizing current is increasing. As the viscosity increases, the shear strength of synthesized MRP fluid also

increases. At the value of 0 A and 1A there is fluctuations in the viscosity of MRP fluid. After 2 A there is change in viscosity is very less against the increase in shear stress. Therefore the viscosity of fluid becomes stable. Initially when the synthesized MRP fluid was sheared, it starts interacting with the rotating parallel plates of the equipment, therefore there is the large reduction in viscosity of synthesized MRP fluid. But after sometime there is very less change in the viscosity of the synthesized MRP fluid. The synthesized MRP fluid has the greater yield strength and stability against the continuous increase in shear rate. Therefore the CIPs hold abrasives more firmly for long interval of time. That is very much required for the finishing of the workpiece. For better finishing it is required to keep the magnetized current 2 A or more than 2 A as there is more stability in viscosity of synthesized MRP fluid. The trend of the current v/s viscosity and the current v/s shear strength is shown in Figures 4.2 and 4.3.

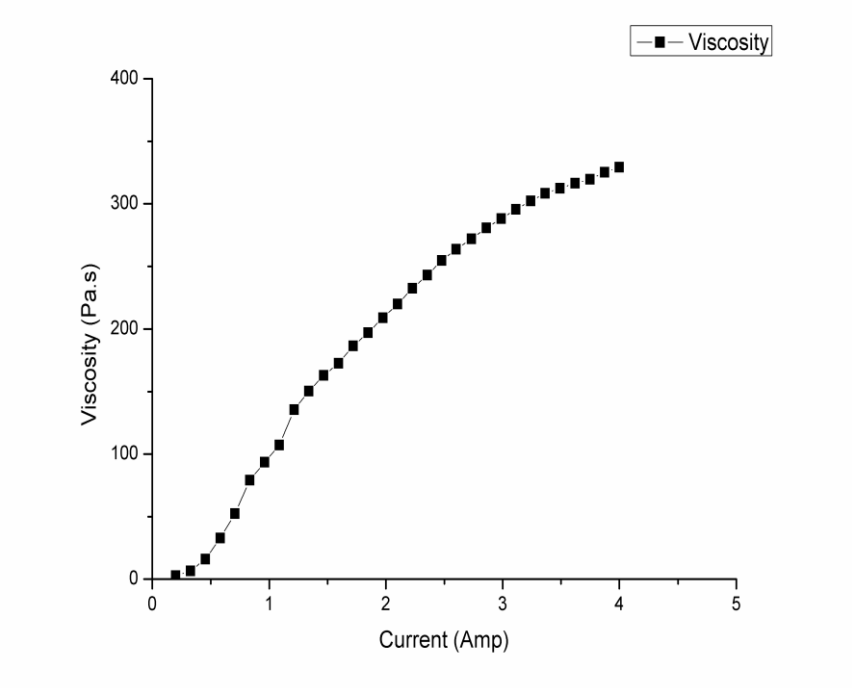

Figure 4.2: Current v/s Viscosity

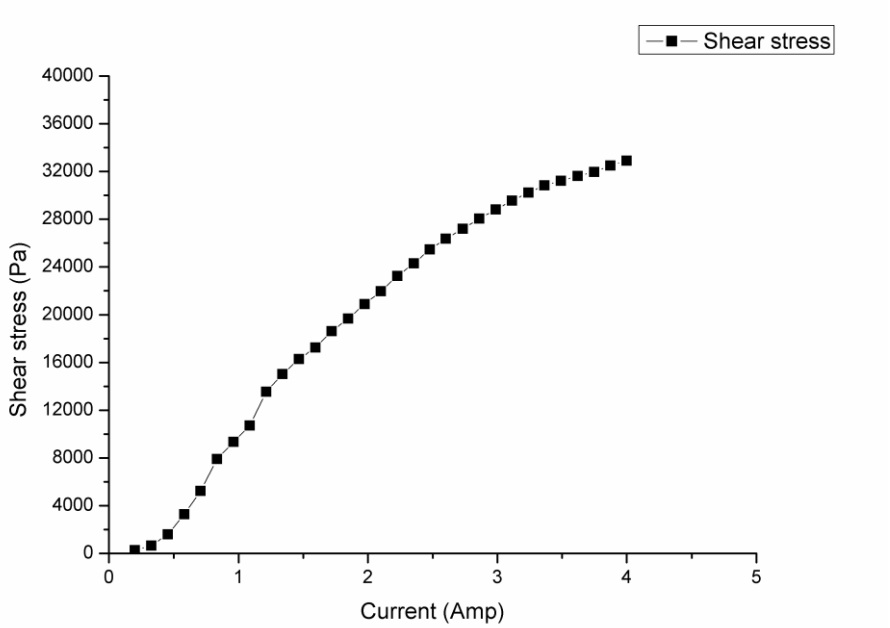

Figure 4.3: Current v/s Shear stress

4.2 Experimental condition for both ferromagnetic and non ferromagnetic workpiece

Table 4.3: Experimental condition for ferromagnetic and non ferromagnetic workpiece

Parameters	Conditions for	
	Mild steel workpiece	Aluminium workpiece
Total finishing time (min)	180	180
Tool rotation (rpm)	75	75
Working gap (mm)	1	0.6
DC power supply to coil	3 A	3A

DC power of 3 A is supplied to the electromagnetic coil of tool by means of slip ring and carbon bushes. Experiments were performed at different interval of times. The variation in the roughness value was calculated at every 30 min of the finishing. Rotational speed was kept 75 rpm for both mild steel and aluminium workpiece. The working for the mild steel was kept 1 mm and for the aluminum working gap was kept 0.6 mm. The MRP fluid with mesh size 800 SIC abrasive powder is used for both mild steel and aluminium workpiece. The concentration of SIC abrasives was kept 25% in the MRP fluid that was used for

finishing of the mild steel and aluminium workpiece. The experiments are conducted at workpiece at the experimental conditions as shown in table 4.3.

4.2.1 Experimentation on ferromagnetic workpiece

The experimentation was performed on the mild steel workpiece with internal diameter 70 mm and height 35 mm. The workpiece was hold by the rectangular workpiece fixture as shown in the Figure 3.28 that was hold by the precision vice on the linear x-y slide. The initial roughness of the mild steel workpiece was 1.90 µm that was obtained by grinding the surface as shown in fig. 4.4. The final roughness after 180 min of MR finishing was 530 nm as shown in Figure 4.5. The surface roughness is measured by the Mitutoyo Surftest 400 with cutoff length 0.25 mm.

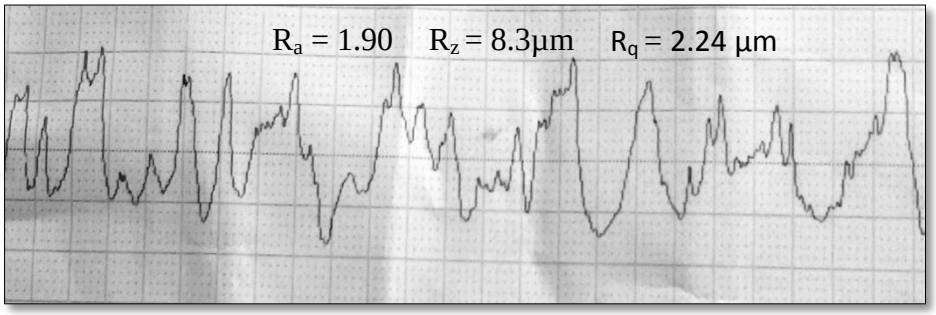

Figure 4.4: Initial surface roughness profile for mild steel workpiece

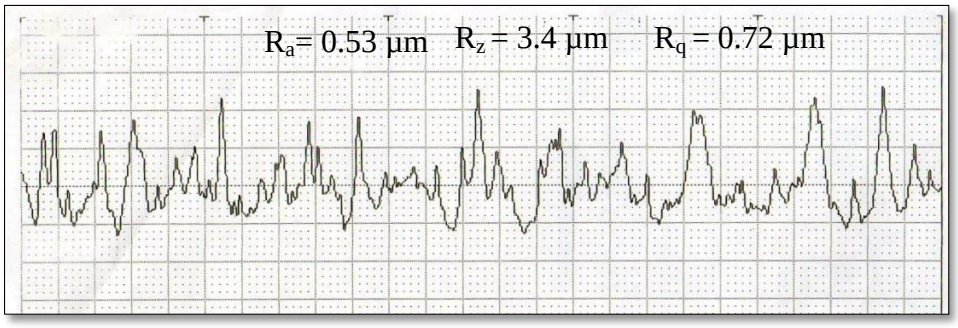

Figure 4.5: Surface roughness profile for mild steel workpiece after 180 min of finishing time

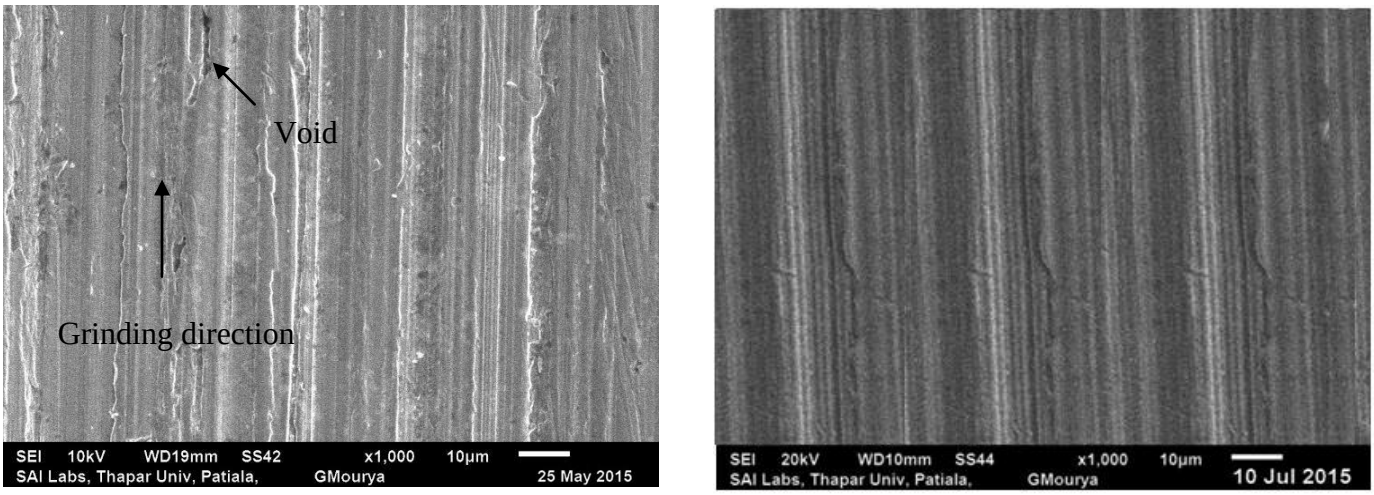

(a) **(b)**

Figure 4.6: SEM micrograph at 1000x (a) before and (b) after 180miutes of MR finishing for mild steel

SEM was conducted for initial and final workpiece. The surface texture of workpiece was evaluated at most excellent finishing situation with SEM at 1000x for initial and final roughness after 180 min. of finishing as shown in Fig 4.6 (a) and (b) respectively. . Significant improvement is measured as compare to initial and final roughness profile.

4.2.2 Experimentation on non ferromagnetic workpiece

The experiments were performed on the aluminium workpiece with internal diameter 69.2 mm and height 35 mm. The initial roughness of the aluminium workpiece was 3.25 µm as shown the Figure 4.7. The final roughness after 180 min of MR finishing was 1.84 µm as shown in Figure 4.8.

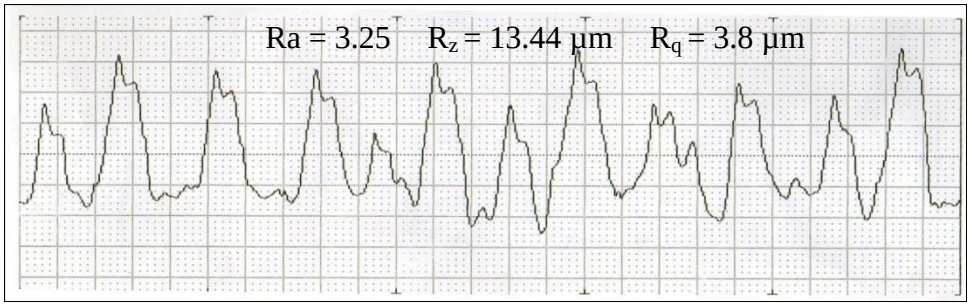

Figure 4.7: Initial surface roughness profile for aluminium workpiece

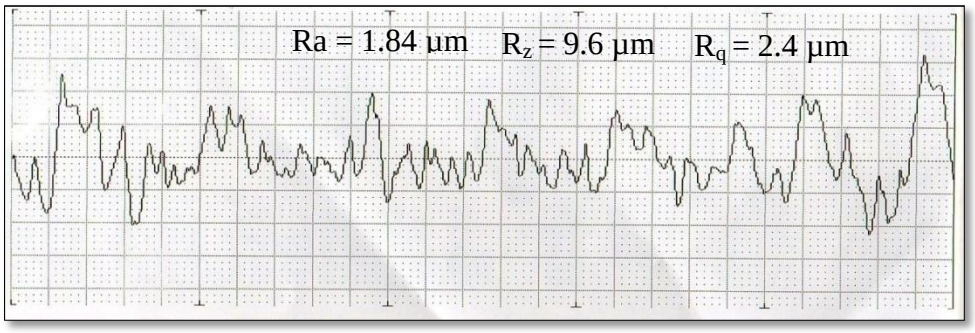

Figure 4.8: Surface roughness profile for aluminium workpiece after 180 min of finishing time

4.3 Results and discussion

The experiments were done on the mild steel and aluminium workpiece to study the outcome of finishing time on the value of surface roughness. The experimental result for change in roughness value for the mild steel with the different interval of time is shown in Figure 4.9. The change in roughness value at different interval of time for aluminium workpiece after 180 min finishing of aluminium workpiece is shown in Figure 4.10.

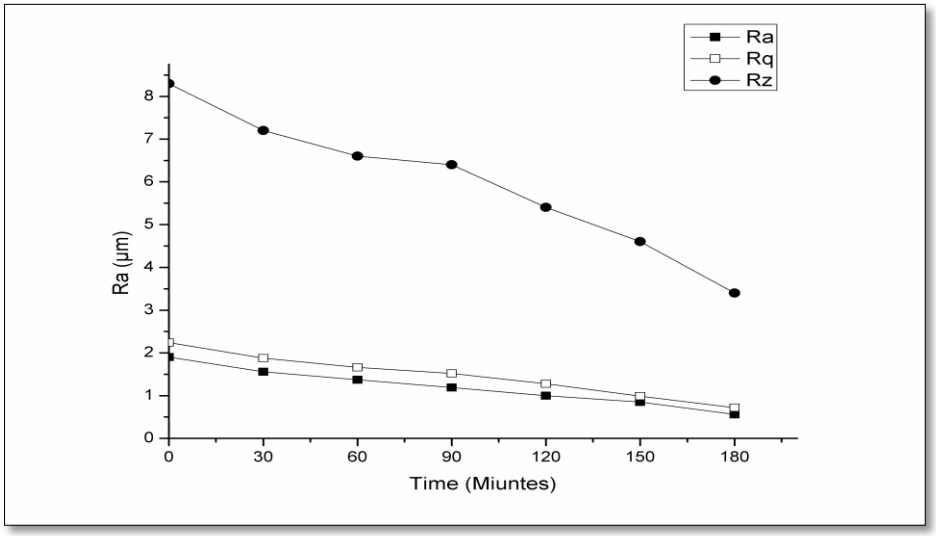

Figure 4.9: Effect of finishing time on the surface roughness value for mild steel workpiece

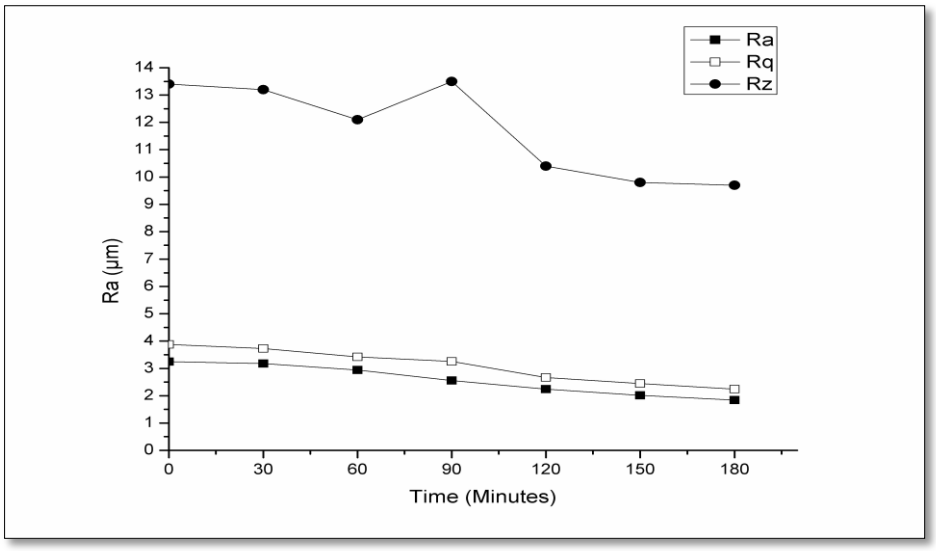

Figure 4.10: Effect of finishing time on the surface roughness value for aluminium workpiece

4.3.1 Observation and discussion for ferromagnetic workpiece

Figure 4.9 shows the effect of finishing time on the surface roughness value of the mild steel workpiece. The roughness value is measured after every 30 min of MR finishing. As shown in Figure 4.9 it is seen that roughness value is decreasing gradually from roughness value 1.90 µm to 530 nm. There for newly developed magnetorheological honing process has the capability to trim down the surface roughness value for the ferromagnetic surface. The roughness profile after 180 min MR finishing for mild steel is shown in Figure 4.5. This is confirming that newly developed magnetorheological honing process is capable for performing the finishing action.

The first experiment was conducted at initial value of 1.90 µm. after 30 min of MR finishing roughness value decreased to 1.56 µm as shown in Figure 4.9. the silicon carbide abrasives has the cutting edges that were hold by the carbonyl iron particles chain move relative to the workpiece surface during the rotation of the magnetorheological honing tool and remove the peaks from the workpiece material. The amount of the material removed depends upon the bonding strength of the carbonyl iron particles and abrasives. The bonding strength of MRP fluid can be controlled by controlling the magnetic field around the magnetorheological honing tool surface by changing the current value and the gap between workpiece and the magnetorheological honing tool. After 30 to 60 min the roughness value changed from 1.56 µm to 1.37 µm. after 180 min of MR finishing roughness value came to 530 nm from 1.9 µm.

thus it is concluded that the newly developed magnetorheological honing process has the capability to finish the ferromagnetic workpiece.

4.3.2 Observation and discussion for non ferromagnetic workpiece

Figure 4.10 shows the result of finishing time on the roughness value of internal surface of cylindrical aluminium workpiece. As shown in the Figure 4.10 it can be seen that roughness value changed from 3.25 µm to 1.84 µm after 180 min of MR finishing. The surface roughness profile of aluminium workpiece after 180 min of MR finishing is shown in Figure 4.8 the improvement in surface roughness value indicates that the newly developed magnetorheological honing process has the capability of finishing the non ferromagnetic workpiece.

From the experiments conducted on both ferromagnetic and non ferromagnetic workpiece it is concluded that newly developed magnetorheological honing process is capable to do finishing of both ferromagnetic and non ferromagnetic surfaces.

Chapter 5

Conclusion and Scope for future work

5.1 Conclusions

- A newly précised magnetorheological honing process is designed and developed.
- FEM analysis for the bracket assembly was done and bracket assembly was safe in terms of static and modal analysis.
- Average roughness value of mild steel workpiece reduces from 1.90 µm to 530 nm and for the aluminium workpiece reduces from 3.25 µm to 1.84 µm after 180 min of MR finishing.
- SEM analysis shows that surface texture is improved after the MR finishing.
- From the experimental results, it was concluded that the newly developed magnetorheological honing process is capable for precise finishing of both ferromagnetic and non ferromagnetic surfaces.

5.2 Scope for future work

- C shape bracket can be used instead of L shape bracket because C shape bracket can improve the vibration characteristics of the magnetorheological honing tool.

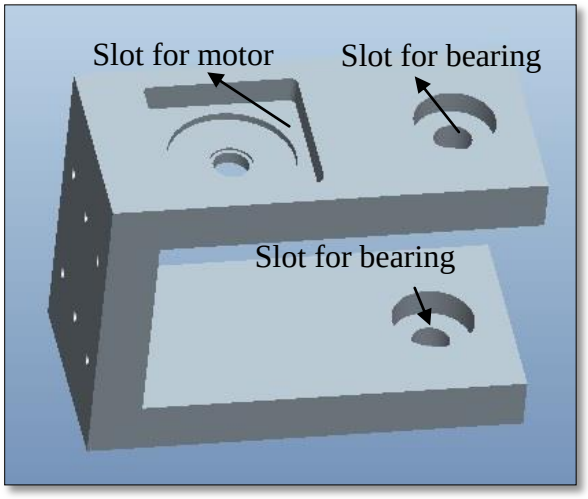

Figure 5.1: CAD model of C shape bracket

- Newly developed Magnetorheological honing process can be used in the finishing of practical applications i.e. bearings, hydraulic cylinders etc.

- Magnetorheological honing process can be used for finishing of different ferromagnetic and non ferromagnetic surfaces i.e. EN 31, copper etc.

References

Bayoumi, M.R.;Abdellatif, A.K. (1995) Effect of surface finish on fatigue strength. Engineering Fracture Mechanics, 51(5): 861-70.

Brecker, J.N., Brown, R., Matsuo, T., Saito, K., Sweeney, J.A., Vansaun, J.B., Shaw, M.C. (1969) Abrasive Grain Association on Investigation of Abrasive Grain Characteristics, 4th Annual Report, Carnegie Institute of Technology, USA.

Cheng, H.; Feng, Y.; Wang, T.; Dong, Z. (2010) Magnetorheological finishing of optical surface combined with symmetrical tool function. Frontiers of Optoelectronics, 3(4): 408-412.

Das, M.; Jain, V.K.; Ghoshdastidar, P.S. (2008) Fluid flow analysis of magnetorheological abrasive flow finishing process. International Journal of Machine Tools and Manufacture, (48): 415-426.

Das, M.; Jain, V.K.; Ghoshdastidar, P.S. (2012) Nano finishing of flat workpiece using rotational magnetorheological abrasive flow finishing process. International Journal of Advanced Manufacturing Technology, (62): 405-420.

Gheisari, R.; Ghasemi, A.A.; Jafarkarimi, M.; Mohtaram, S. (2014) Experimental studies on the ultraprecision finishing of cylindrical surfaces using magnetorheological finishing process. Production & Manufacturing Research, 2:1: 550-557.

Hong, K.P.; Cho, Y.K.; Shin, B.C.; Cho, M.W.; Choi, S.B.; Cho, W.S.; Jae, J.J. (2012) MR fluid polishing of Alumina reinforced zirconia ceramics using diamond abrasive for dental application. Materials and Manufacturing Processes, (27): 1135-1138.

Jain, V.K. (2009) Magnetic field assisted abrasive based micro-/nano-finishing. Journal of Materials Processing Technology (209):6022-6038.

Jha, S., Jain, V.K. (2004) Design and development of the magnetorheological abrasive flow finishing (MRAFF) process, International Journal of Machine Tools and Manufacture (44), 1019-1029.

Jha, S.; Jain, V.K. (2006) Modeling and simulation of surface roughness in magnetorheological abrasive flow finishing process. Wear, (261): 856-866.

Jha, S.; Jain, V.K.; Komanduri, R. (2007) Effect of extrusion pressure and number finishing cycles on the surface roughness in Magnetorheological abrasive flow finishing process. International Journal of Advanced Manufacturing Technology, (33): 725-729.

Judal, K.B.; Yadava, V.; Pathak, D. (2013) Experimental investigation of vibration assisted cylindrical magnet abrasive finishing of Aluminium workpiece. Materials and Manufacturing Processes, (28): 1196-1202.

Kang, J.; George, A.; Yamaguchi, H. (2012) High-speed internal finishing of capillary tubes by magnetic abrasive finishing. Procedia CIRP, (1): 414-418.

Kordonski, W.I., Golini, D. (1999) Fundamentals of magnetorheological fluid utilization in high precision finishing, Journal of Intelligent Material Systems and Structures 10(9):683-689.

Kordonski, W.I.; Shorey, A.B.; Tricard, M. Nov (2004) Magnetorheological (MR) jet finishing technology. Proceeding of ASME International Mechanical Engineering Congress, 13-19: 1-8.

Lam, S.Y. (2000) Process monitoring of abrasive flow machining using a neural network predictive model, Technical paper, University of Pittsburgh: Pittsburgh, PA.

Jain, V.K. (2009) Magnetic field assisted abrasive based micro-/nano-finishing. Journal of material processing technology, (209): 6022-6038

Mori, Y., Yamauchi, K., Endo, K. (1987) Elastic Emission machining. Precision Engineering , (3):123-128.

Rhoades, L.J. (1988) Abrasive flow machining, Manufacturing Engineering, (1): 75-78.

Sadiq, A. Shunmugan, M.S. (2010) A novel method to improve finish on non-magnetic surface in magnetorheological abrasive honing process. Tribology International (43):1122-1126.

Sadiq, A., Shunmugan, M.S. (2009) Investigation into magnetorheological abrasive honing. International Journal of Machine Tools and Manufacture (49):554-560.

Shankar, R.M.; Jain, V.K.; Ramkumar, J. (2010) Rotational abrasive flow finishing process and its effects on finished surface topography. International Journal of Machine Tools and Manufacture, (50): 637-650.

Sidpara, A.; Jain, V.K. (2011) Experimental investigations into forces during magnetorheological fluid based finishing process. International Journal of Machine Tools and Manufacture, (51): 358-362.

Singh, A.K.; Jha, S.; Pandey, P.M. (2011) Design and development of nanofinishing process for 3D surfaces using ball end MR finishing tool. International Journal of Machine Tools and Manufacture, (51):142-151.

Singh, A.K.; Jha,S.; Pandey, P.M. (2013) Rheological behaviour of MR polishing fluid in ball end magnetorheological finishing process. Magnetohydrodynamics,(49): 512-515

Uhlmann, E.; Doits, M.; Schmiedel, C. (2013) Development of a material model for visco-elastic abrasive medium in Abrasive Flow Machining. Procedia CIRP, (8): 351-356.

Yamaguchi, H.; Shinmura, T. (2004) internal finishing process for alumina ceramic components by a magnetic field assisted finishing process. Precision Engineering, (28): 135-142.

Zantye, P.B.; Kumar, A.; Sikder, A.K. (2004) Chemical mechanical planarization for micro-electronics applications. Material Science and Technology R, (45): 89-220.

Web References

matweb.com/search/propertysearch.aspx

http://www.columbiagrinding.com/lapping.html